Journal of Medicinal Chemistry

Article

Pyrido[2,3-*e*]-1,2,4-triazolo[4,3-*a*]pyrazin-1-one as a New Scaffold To Develop Potent and Selective Human A Adenosine Receptor Antagonists. Synthesis, Pharmacological Evaluation, and Ligand#Receptor Modeling Studies

Vittoria Colotta, Ombretta Lenzi, Daniela Catarzi, Flavia Varano, Guido Filacchioni, Claudia Martini, Letizia Trincavelli, Osele Ciampi, Anna Maria Pugliese, Chiara Traini, Felicita Pedata, Erika Morizzo, and Stefano Moro

J. Med. Chem., **2009**, 52 (8), 2407-2419• DOI: 10.1021/jm8014876 • Publication Date (Web): 20 March 2009

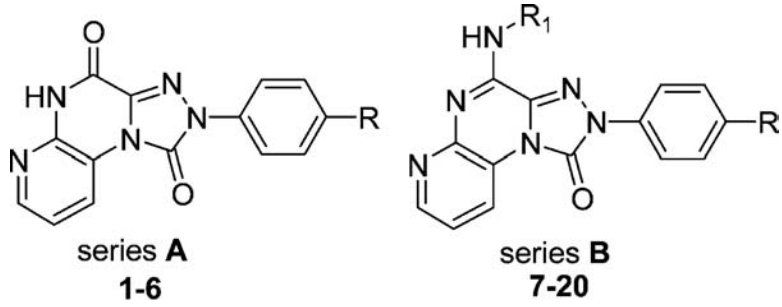

More About This Article

Additional resources and features associated with this article are available within the HTML version:

- Supporting Information
- Access to high resolution figures
- Links to articles and content related to this article
- Copyright permission to reproduce figures and/or text from this article

View the Full Text HTML

Pyrido[2,3-*e*]-1,2,4-triazolo[4,3-*a*]pyrazin-1-one as a New Scaffold To Develop Potent and Selective Human A_3 Adenosine Receptor Antagonists. Synthesis, Pharmacological Evaluation, and Ligand−Receptor Modeling Studies

Vittoria Colotta,*[,†] Ombretta Lenzi,[†] Daniela Catarzi,[†] Flavia Varano,[†] Guido Filacchioni,[†] Claudia Martini,[‡] Letizia Trincavelli,[‡] Osele Ciampi,[‡] Anna Maria Pugliese,[§] Chiara Traini,[§] Felicita Pedata,[§] Erika Morizzo,[||] and Stefano Moro[||]

Laboratorio di Progettazione, Sintesi e Studio di Eterocicli Biologicamente Attivi, Dipartimento di Scienze Farmaceutiche, Università di Firenze, Polo Scientifico, Via Ugo Schiff, 6, 50019 Sesto Fiorentino, Italy, Dipartimento di Psichiatria, Neurobiologia, Farmacologia e Biotecnologie, Università di Pisa, Via Bonanno, 6, 56126 Pisa, Italy, Dipartimento di Farmacologia Preclinica e Clinica, Università di Firenze, Viale Pieraccini 6, 50139 Firenze, Italy, and Molecular Modeling Section (MMS), Dipartimento di Scienze Farmaceutiche, Università di Padova, Via Marzolo 5, 35131 Padova, Italy

Received November 26, 2008

The paper describes a new class of human (h) A_3 adenosine receptor antagonists, the 2-arylpyrido[2,3-*e*]-1,2,4-triazolo[4,3-*a*]pyrazin-1-one derivatives (PTP), either 4-oxo (**1**−**6**, series **A**) or 4-amino-substituted (**7**−**20**, series **B**). In both series **A** and **B**, substituents able to act as hydrogen bond acceptors (OMe, OH, F, COOEt) were inserted on the 2-phenyl ring. In series **B**, cycloalkyl and acyl residues were introduced on the 4-amino group. Some of the new derivatives showed high hA_3 AR affinities (K_i < 50 nM) and selectivities vs both hA_1 and hA_{2A} receptors. The selected 4-benzoylamino-2-(4-methoxyphenyl)pyrido[2,3-*e*]-1,2,4-triazolo[4,3-*a*]pyrazin-1-one (**18**), tested in an in vitro rat model of cerebral ischemia, proved to be effective in preventing the failure of synaptic activity induced by oxygen and glucose deprivation in the hippocampus. Molecular docking of this new class of hA_3 AR antagonists was carried out to depict their hypothetical binding mode to our refined model of hA_3 receptor.

Introduction

Adenosine is well recognized as an important neuromodulator that affects a large variety of physiopathological functions through activation of at least four specific cell surface receptors, termed A_1, A_{2A}, A_{2B}, A_3, which belong to the G-protein-coupled receptor family.[1,2] Stimulation of adenosine receptors (ARs[a]) inhibits (A_1 and A_3) or activates (A_{2A} and A_{2B}) adenylyl cyclase, thus decreasing or increasing, respectively, cAMP production.[2] Other second messenger signaling pathways have been described. A positive modulation of phospholipase C[3] and D[4] and K_{ATP} channels[5] has been reported for the A_3 AR that also couples to members of the mitogen-activated protein kinase (MAPK) family, such as the extracellular signal-regulated kinase (ERK) 1/2 and p38.[6] Modulation of MAPK is thought to have a role in the effects that the A_3 AR elicits on cell growth, survival, and death.[6,7] Growing evidence indicates that A_3 AR antagonists could have therapeutic potential in renal injury,[8] in the treatment of glioblastoma multiforme,[9] and as antiglaucoma agents.[10] Recently, A_3 AR antagonists have also been described as potential neuroprotective agents in ischemia- and aging-associated brain damages.[7,11−14] Nevertheless, studies regarding the role of the A_3 AR receptor in the pathophysiology of cerebral ischemia have provided contrasting results. In fact, it has been proven that A_3 receptor activation can induce both cell protection and cell damage, depending on the degree of receptor activation and/or the cell type.[6,7,14]

In the past years much of our research has been directed toward the discovery of potent and selective hA_3 AR antagonists belonging to different heterocyclic classes,[13,15−24] and among them the 2-aryl-1,2,4-triazolo[4,3-*a*]quinoxalin-1-one derivatives (TQX), either 4-oxo- or 4-amino-substituted, have been deeply investigated (Chart 1).[15−19,22−24] On the basis of the observed structure−affinity relationships (SAR) in the TQX compounds, a new class of AR antagonists was designed, synthesized, and pharmacologically tested: the 2-aryl-pyrido[2,3-*e*]-1,2,4-triazolo[4,3-*a*]pyrazin-1-one derivatives (PTP), 6-aza analogues of TQX (Chart 1).

Rational Design of the Pyrido[2,3-*e*]-1,2,4-triazolo[4,3-*a*]pyrazin-1-one Derivatives

An intensive study of the SAR in the 2-aryltriazoloquinoxalin-1-one derivatives TQX led to the identification of some substituents (R, R_1, R_6) which, introduced one by one in a suitable position, generally afforded high hA_3 affinity and selectivity[15,16,22] (Chart 1). These substituents are the *p*-methoxy (R) on the 2-phenyl ring, the nitro group (R_6) at the 6-position (4-oxo and 4-amino series), and acyl residues (R_1) on the 4-amino group (4-amino series). Even best results, in terms of hA_3 affinity and especially of selectivity, ensued from the combination of R = OMe with $R_6 = NO_2$ or with R_1 = acyl.[19,22]

* To whom correspondence should be addressed. Phone: +39 55 4573731. Fax: +39 55 4573780. E-mail: vittoria.colotta@unifi.it.

† Dipartimento di Scienze Farmaceutiche, Università di Firenze.

‡ Università di Pisa.

§ Dipartimento di Farmacologia Preclinica e Clinica, Università di Firenze.

|| Università di Padova.

[a] Abbreviations: GPCRs, G-protein-coupled receptors; AR, adenosine receptor; cAMP, cyclic adenosine monophosphate; MAPK, mitogen-activated protein kinase; ERK, extracellular signal-regulated kinase; h, human; SAR, structure−affinity relationship; r, rat; DPCPX, 8-cyclopentyl-1,3-dipropylxanthine; CGS 21680, 2-[4-(2-carboxyethyl)phenethyl]amino-5′-(*N*-ethylcarbamoyl)adenosine; I-AB-MECA, N^6-(4-amino-3-iodobenzyl)-5′-(*N*-methylcarbamoyl)adenosine; NECA, 5′-(*N*-ethylcarboxamido)adenosine; C1-IB-MECA, 2-chloro-N^6-(3-iodobenzyl)-5′-(*N*-methylcarbamoyl)adenosine; TM, transmembrane; RBHM, rhodopsin-based homology modeling; LBHM, ligand-based homology modeling; EL2, second extracellular loop; MOE, molecular operating environment; OGD, oxygen and glucose deprivation; AD, anoxic depolarization; fEPSP, field excitatory postsinaptic potential; dc, direct current; aCSF, artificial cerebral spinal fluid.

10.1021/jm8014876 CCC: $40.75
Published on Web 03/20/2009

Chart 1. Previously Reported 2-Aryl-1,2,4-triazolo[4,3-*a*]quinoxalin-1-one Derivatives (TQX) and Newly Synthesized 2-Arylpyrido[2,3-*e*]-1,2,4-triazolo[4,3-*a*]pyrazin-1-one Bioisosters (PTP)

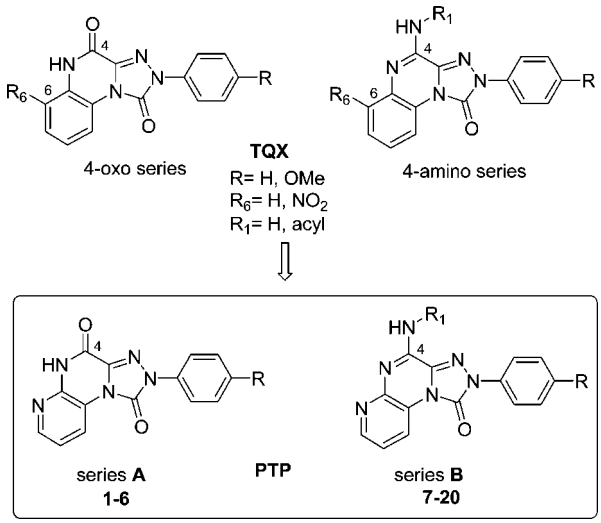

Instead, when $R_6 = NO_2$ was combined with R_1 = acyl, not always a good hA_3 affinity was obtained.[22,24] The same applies when the three substituents R, R_1, and R_6 were simultaneously introduced in the key positions.[22] Molecular modeling studies permitted depiction of the putative binding motif of these derivatives on a refined model of the hA_3 AR and to rationalize the observed SAR.[19,22,24] At least two hydrogen-bonding interactions stabilize the anchoring of the tricyclic scaffold inside the binding cleft: one involving the 1-carbonyl group and the other the 4-oxo/4-amino function. Additional hydrogen bonds can be engaged by the nitro group in R_6, the methoxy in R, and the acyl carbonyl group in R_1, thus explaining the positive effects of these substituents for the hA_3 AR affinity. Both the 2-aryl and the fused benzo rings are positioned in two size-limited hydrophobic pockets, and as a consequence, the volume of the whole molecule is critical in the fitting with the receptor. For the 4-amino series it has been found that the bulkiness of the R_1 acyl residue plays a key role in the fine control of the orientation of the molecule in the binding site and that it influences the positioning of the 6-nitro substituent that does not always exert a profitable effect.[22,24] The unfavorable steric interactions of the nitro group with the receptor site have been thought to be responsible for the reduction of affinity of some 6-nitro-4-amido-substituted derivatives. On this basis, we designed a new series of AR antagonists deriving from the replacement of the 6-nitro group of the 1,2,4-triazolo[4,3-*a*]quinoxalin-1-one derivatives with an endocyclic nitrogen atom that could act as hydrogen-bond acceptor without hindering anchoring to the receptor site. Thus, applying the isosteric replacement of the nitrobenzene moiety with a pyridine ring, the 6-aza analogues of the TQX derivatives, namely, the 2-arylpyrido[2,3-*e*]-1,2,4-triazolo[4,3-*a*]pyrazin-1-one derivatives (PTP, Chart 1), both 4-oxo (**1**−**6**, series **A**) and 4-amino-substituted (**7**−**20**, series **B**), were synthesized. In both series **A** and **B**, besides introducing the *p*-methoxy group on the 2-phenyl ring, other substituents able to act as hydrogen bond acceptors (OH, F, COOEt) were inserted. In series **B**, cycloalkyl and acyl residues were introduced on the 4-amino group. The new derivatives **1**−**20** were tested to evaluate their affinities at ARs, and one selected compound (**18**) was also tested in an in vitro rat model of cerebral ischemia, since in a previous study[24] a TXQ derivative proved to be effective in preventing the failure of synaptic activity induced by oxygen and glucose deprivation in the hippocampus.

Molecular docking of this new class of hA_3 AR antagonists was carried out to depict their hypothetical binding mode to our refined model of hA_3 receptor.

Scheme 1[a]

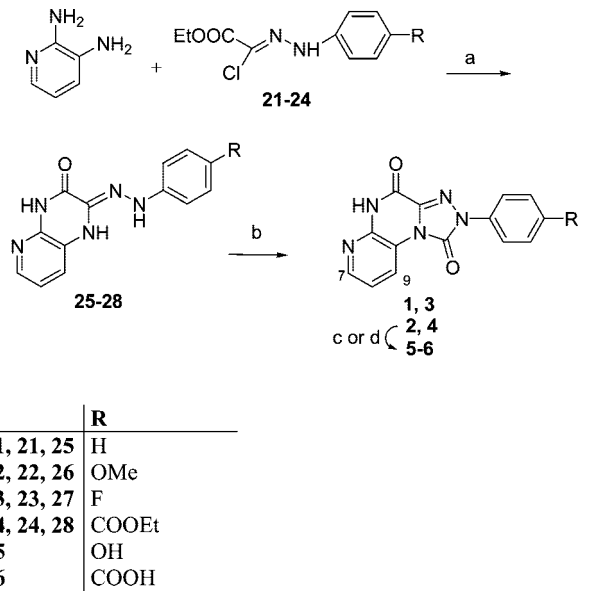

	R
1, 21, 25	H
2, 22, 26	OMe
3, 23, 27	F
4, 24, 28	COOEt
5	OH
6	COOH

[a] (a) Et_3N, EtOH; (b) $(Cl_3CO)_2CO$, THF; (c) 48% HBr, AcOH; (d) (i) 0.8 N NaOH/EtOH; (ii) 6 N HCl.

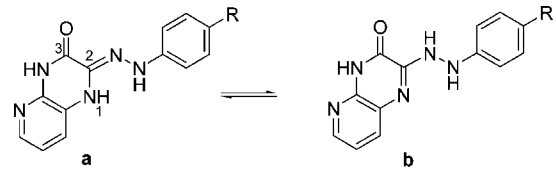

Figure 1. Two tautomeric forms of intermediates **25**−**28**.

Chemistry

The target pyrido[2,3-*e*]-1,2,4-triazolo[4,3-*a*]pyrazin-1-one derivatives **1**−**20** were prepared as outlined in Schemes 1−3. Scheme 1 shows the synthesis of the 2-arylpyrido[2,3-*e*]-1,2,4-triazolo[4,3-*a*]pyrazin-1,4-diones **1**−**6** which were synthesized by reacting the commercially available 2,3-diaminopyridine with a suitable ethyl N^1-arylhydrazono-N^2-chloroacetate **21**−**24**.[25−27] From the reaction, the 2-arylhydrazono-1,2-dihydropyrido[2,3-*b*]pirazin-3(4*H*)-ones **25**−**28** were isolated in high yields. These derivatives resulted from the displacement of the chlorine atom of compounds **21**−**24** by the more nucleophilic amino group of the 2,3-diaminopyridine and subsequent cyclization at ester function level. The intermediates **25**−**28** may exist in two tautomeric forms (Figure 1). Indeed, their ^{1}H NMR spectra reveals the existence of both tautomers because there are more than three protons that exchange with D_2O. In compounds **26** (R = OMe) and **28** (R = COOEt) the existence of both species **a** and **b** is also revealed by the presence of doubled signals for the methoxy and carbethoxy substituents. The 2-arylhydrazono structure of derivatives **25**−**28** was assigned on the basis of the ^{1}H NMR spectra of the corresponding tricyclic derivatives **1**−**4**, obtained from **25**−**28** and triphosgene (Scheme 1). In the ^{1}H NMR spectra of **1**−**4** the signal of the two most deshielded protons appears as a doublet at 8.83−8.84 ppm and at 8.33−8.35 ppm with, respectively, a coupling constant of about 8.1 and

Scheme 2[a]

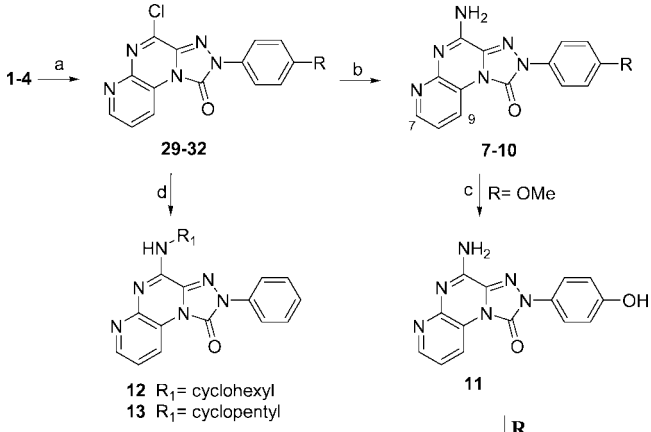

	R
7, 29	H
8, 30	OMe
9, 31	F
10, 32	COOEt

[a] (a) $PCl_5/POCl_3$, pyridine; (b) NH_3(g), absolute EtOH; (c) 48% HBr, AcOH; (d) NH-R_1, absolute EtOH.

Scheme 3[a]

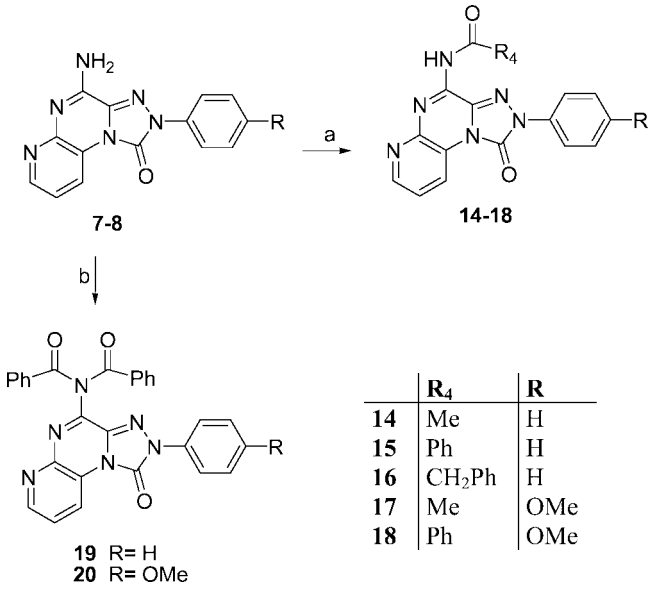

	R_4	R
14	Me	H
15	Ph	H
16	CH_2Ph	H
17	Me	OMe
18	Ph	OMe

[a] (a) R_4COCl, anhydrous pyridine; (b) excess of PhCOCl, anhydrous pyridine.

4.8 Hz, this latter value being typical of a 2-pyridine proton. Thus, considering both the chemical shifts and the *J* values, the second signal was assigned to the H-7 proton and the first to the H-9, this latter proton being more deshielded because of the paramagnetic effect of the 1-carbonyl group. Indeed, compounds **1**−**4**, and consequently **25**−**28**, were pyrido[2,3-*b*]pirazino derivatives.

Demethylation of the 2-(4-methoxyphenyl) derivative **2** afforded the 2-(4-hydroxyphenyl) compound **5**. From alkaline hydrolysis of the ethyl carboxylic ester **4**, the corresponding carboxylic acid **6** was obtained. The 4-amino-2-arylpyrido[2,3-*e*]-1,2,4-triazolo[4,3-*a*]pyrazin-1-ones **7**−**11** and the 4-cycloalkyamino derivatives **12**, **13** were synthesized as depicted in Scheme 2. The 1,4-dione derivatives **1**−**4** were reacted with phosphorus pentachloride and phosphorus oxychloride to give the corresponding 4-chloro derivatives **29**−**32** which were transformed into the desired 4-amino-substituted compounds **7**−**10** with ammonia. The 2-(4-hydroxyphenyl) derivative **11** was prepared by demethylation of the 2-(4-methoxyphenyl) derivative **8**. The 4-cycloalkylamino derivatives **12** and **13** were prepared by reacting the 4-chloro derivative **7** with, respectively, cyclohexylamine and cyclopentylamine. The 4-amido derivatives **14**−**20** were obtained as illustrated in Scheme 3. Reaction of the 4-amino derivatives **7** and **8** with the suitable acyl chlorides gave the corresponding 4-amido-substituted compounds **14**−**18**, while from treatment of **7** and **8** with an excess of benzoyl chloride the 4-dibenzoylamino derivatives **19** and **20** were obtained, respectively.

Pharmacology

Compounds **1**−**20**, rationally designed to obtain hA_3 receptor antagonists, were tested for their ability to displace [^{125}I]N^6-(4-amino-3-iodobenzyl)-5′-(*N*-methylcarbamoyl)adenosine ([^{125}I]AB-MECA) from cloned hA_3 receptor stably expressed in CHO cells. Subsequently, the selected compounds **1**, **2**, **8**, **12**−**18**, and **20**, which showed the highest A_3 AR affinities ($K_i \leq 250$ nM), were tested for their ability to displace [^{3}H]DPCPX from cloned hA_1 ARs and [^{3}H]5′-(*N*-ethylcarboxamido)adenosine ([^{3}H]NECA) from cloned hA_{2A} ARs, to establish their hA_3 selectivities both vs hA_1 and hA_{2A} ARs.

Compounds **1**−**20** were also tested at the bovine (b) A_1 AR, from cerebral cortical membranes, and at the bA_{2A} AR, from striatal membranes, using respectively [^{3}H]8-cyclopentyl-1,3-dipropylxanthine ([^{3}H]DPCPX) and [^{3}H]2-[4-(2-carboxyethyl)phenethyl]amino-5′-(*N*-ethylcarbamoyl)adenosine ([^{3}H]CGS 21680) as radioligands.

The binding results of **1**−**20**, together with those of theophylline and DPCPX included as antagonist reference compounds, are reported in Table 1.

Compound **18**, which showed the highest hA_3 affinity and selectivity among the herein reported compounds, both vs hA_1 and hA_{2A} ARs, was selected for further investigations. It was tested at the hA_{2B} receptor by evaluating its inhibitory effect on NECA-stimulated cAMP levels in hA_{2B} CHO cells. The same functional assay was performed on hA_3 CHO cells in order to assess the antagonism of compound **18** on 2-chloro-N^6-(3-iodobenzyl)-5′-(*N*-methylcarbamoyl)adenosine (Cl-IB-MECA)-inhibited cAMP production. Moreover, rat (r) A_1, A_{2A}, and A_3 AR affinities were evaluated using [^{3}H]DPCPX (rat cortex), [^{3}H]CGS 21680 (rat striatum), and [^{125}I]AB-MECA (HEK cells stably transfected with the rat A_3 receptor).

Compound **18** was selected to evaluate its effect in an in vitro rat model of cerebral ischemia obtained by oxygen and glucose deprivation (OGD).

Results and Discussion

(A) Structure−**Affinity Relationship Studies.** The hA_3 AR binding data, reported in Table 1, show that the pyrido[2,3-*e*]-1,2,4-triazolo[4,3-*a*]pyrazin-1-one tricyclic system is a new scaffold to obtain potent and selective hA_3 AR antagonists. In fact, some of the novel derivatives showed high hA_3 AR affinities ($K_i < 50$ nM) and selectivities vs hA_1 (compounds **2**, **12**, **13**, **16**−**18**, **20**) and vs hA_{2A} (**2**, **17**, **18**, **20**) receptors. Good affinity for the hA_{2A} receptor was observed for compounds **12**, **13**, and **16**.

This new class of AR antagonists and their triazoloquinoxaline leads share common SAR at the hA_3 receptor. First of all is the profitable effect of the *p*-methoxy substituent on the 2-phenyl ring. In fact, this substituent increases the hA_3 affinity, both in the 4-oxo series (compare compound **2** to **1**) and in the 4-amino series (compare compound **8** to **7**), as previously described for the leads.[15,19] The 2-(4-methoxyphenyl)-4-one

Table 1. Binding Affinity at Human A_1, A_{2A}, A_3 and Bovine A_1 and A_{2A} ARs

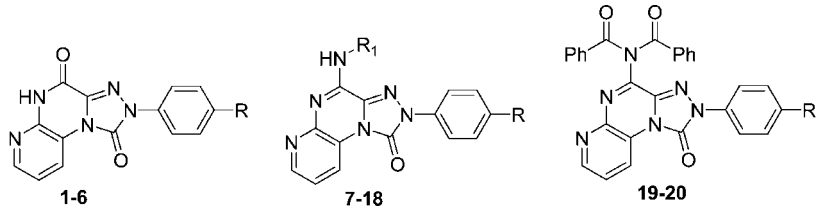

			K_i[a] (nM) o I %				
	R_1	R	hA_3[b]	bA_1[c]	bA_{2A}[d]	hA_1[e]	hA_{2A}[e]
1		H	251 ± 16	145 ± 11	12%		
2		4-OMe	3.3 ± 0.2	26%	0%	114 ± 8	0%
3		4-F	590 ± 42	305.5 ± 25	26%		
4		4-COOEt	0%	16%	0%		
5		4-OH	32%	449 ± 25	0%		
6		4-COOH	0%	30%	7%		
7	H	H	656 ± 41	3.1 ± 0.28	92.6 ± 5.6		
8	H	4-OMe	158 ± 9.8	1102 ± 81	413 ± 34		
9	H	4-F	490 ± 36	181 ± 15	1508 ± 130		
10	H	4-COOEt	0%	39%	17%		
11	H	4-OH	1335 ± 112	112 ± 8.1	832 ± 62		
12		H	15.5 ± 1.2	0.38 ± 0.029	199 ± 13	37%	211 ± 8.4
13		H	8.4 ± 0.9	0.47 ± 0.047	510 ± 36	36%	208 ± 10
14	COMe	H	138 ± 12	14 ± 1.1	59%		
15	COPh	H	70.3 ± 6	152 ± 10	7100 ± 550	8%	2240 ± 230
16	$COCH_2Ph$	H	11.7 ± 1	7.15 ± 0.5	414 ± 32	37%	208 ± 6.2
17	COMe	4-OMe	41 ± 3.2	56%	19%	48%	29%
18	COPh	4-OMe	4.54 ± 0.2	355 ± 22	7%	38%	27%
19		H	335 ± 28	70.7 ± 6.5	12%		
20		4-OMe	7.75 ± 0.8	17%	0%	0%	0%
Theophylline			86000 ±7800	3800 ± 340	21000 ± 1800	6200 ± 530	7900 ± 630
DPCPX			1300 ± 125	0.5 ± 0.03	337 ± 28	3.2 ± 0.2	260 ± 18

[a] The K_i values are mean values ± SEM of four separate assays, each performed in triplicate. [b] Displacement of specific [^{125}I]AB-MECA binding at human A_3 receptors expressed in CHO cells or percentage of inhibition (I%) of specific binding at 1 μM concentration. [c] Displacement of specific [^{3}H]DPCPX and [^{3}H]NECA binding at, respectively, hA_1 and hA_{2A} receptors expressed in CHO cells or percentage of inhibition (I%) of specific binding at 10 μM concentration. [d] Displacement of specific [^{3}H]DPCPX binding in bovine brain membranes or percentage of inhibition (I%) of specific binding at 20 μM concentration. [e] Displacement of specific [^{3}H]CGS 21680 binding from bovine striatal membranes or percentage of inhibition (I%) of specific binding at 20 μM concentration.

derivative **2** also showed good hA_3 selectivity vs both hA_1 and, especially, hA_{2A} receptors. Replacement of the methoxy group of derivatives **2** and **8** with a hydroxy group (compounds **5** and **11**), a fluorine atom (compounds **3** and **9**), and carboxy acid/ester groups (compounds **4**, **6**, **10**) caused a significant drop of the hA_3 affinity. Introduction of a cyclohexyl or a cyclopentyl moiety on the 4-amino group of derivative **7** significantly increases the hA_3 affinity (compounds **12** and **13**, respectively), as in the triazoloquinoxaline-1-one class,[15] and also affords high selectivity vs the hA_1 receptor. Similarly, when acyl groups were appended on the 4-amino substituent of **7** (derivatives **14**−**16**, **19**), a significant gain in the hA_3 affinity, linked to the steric hindrance of the acyl moiety, was obtained. In particular, the benzoyl (compound **15**) and phenylacetyl groups (compound **16**) resulted in being the most advantageous and conferred high hA_3 vs hA_1 selectivity as well. Also in the 4-amido-substituted derivatives, introduction of the *p*-methoxy group on the 2-phenyl ring ameliorated both the affinity and selectivity for the hA_3 receptor, as can be observed by comparing the binding data of compounds **17**, **18**, and **20** to those of derivatives **14**, **15**, and **19**, respectively.

Finally, it is pointed out that the nitrobenzene moiety of the TQX derivatives can be conveniently replaced by the pyridine ring to afford the PTP derivatives as a new class of hA_3 AR antagonists. In fact, as appears evident comparing the binding data of some new derivatives to those of the corresponding triazoloquinoxalines (Table 2), the PTP compounds showed similar (**1**, **2**, **5**, **15**) or even higher (**11**−**14**, **17**−**20**) hA_3 affinities with respect to those of the corresponding 6-NO_2 TQX derivatives.

Among the new PTP compounds, the 4-benzoylamino-2-(4-methoxyphenyl)pyridotriazolopyrazin-1-one derivative **18** possesses the highest hA_3 affinity (K_i = 4.54 nM) and selectivity vs both hA_1 and hA_{2A} receptors. To determine also its hA_3 vs hA_{2B} selectivity we tested compound **18** in cAMP assays which evidenced a lack of hA_{2B} affinity, being that **18** is ineffective in inhibiting NECA-stimulated cAMP levels in hA_{2B} CHO cells (IC_{50} > 10 000). Furthermore, the effect of compound **18** in limiting the NECA-inhibited cAMP accumulation in hA_3 CHO cells was determined. Coherently with its high hA_3 affinity, derivative **18** proved to be very potent in this test, showing an antagonistic behavior (Figure 2, EC_{50} = 36.3 ± 3.1 nM). Since compound **18** was tested in an in vitro rat model of cerebral ischemia, its binding affinities for the rA_1, A_{2A}, and A_3 receptors were measured. The rA_1 affinity value (K_i = 587 ± 58 nM) was similar to the bA_1 one, while the affinities for the rA_{2A} and rA_3 receptors were, respectively, very low (I% at 10 μM = 34) and null (I% at 1 μM = 0).

Before discussion of the binding data at the bA_1 and bA_{2A} receptors, it is pointed out that the choice of testing the PTP

Table 2. Comparison between the hA_3 AR Affinities of the Pyridotriazolopyrazin-1-ones (X = N) and the Corresponding 6-Nitrotriazoloquinoxalin-1-ones (X = C-NO_2)

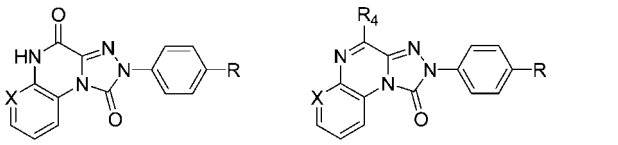

R	R_4	X = N[a]	K_i (nM) hA_3 or I% (1 μM)	X = C-NO_2[b]	K_i (nM) hA_3 or I% (1 μM)
H		**1**	251 ± 16	**33**	279 ± 16
OMe		**2**	3.3 ± 0.2	**34**	4.7 ± 0.52
OH		**5**	32%	**35**	21%
H	H	**7**	656 ± 41	**36**	4.75 ± 0.3
OMe	H	**8**	158 ± 9.8	**37**	47 ± 1.2
OH	H	**11**	1335 ± 112	**38**	45%
H	NHC_6H_{11}	**12**	15.5 ± 1.2	**39**	281 ± 24
H	NHC_5H_9	**13**	8.4 ± 0.9	**40**	116 ± 24
H	NHCOMe	**14**	138 ± 12	**41**	18%
H	NHCOPh	**15**	70.3 ± 6	**42**	22 ± 2.60
OMe	NHCOMe	**17**	41 ± 3.6	**43**	36%
OMe	NHCOPh	**18**	4.54 ± 0.2	**44**	217 ± 20
H	$N(COPh)_2$	**19**	335 ± 22	**45**	27%
OMe	$N(COPh)_2$	**20**	7.75 ± 0.8	**46**	342 ± 21

[a] Data from Table 1. [b] Data from refs 16, 18, 19, and 22.

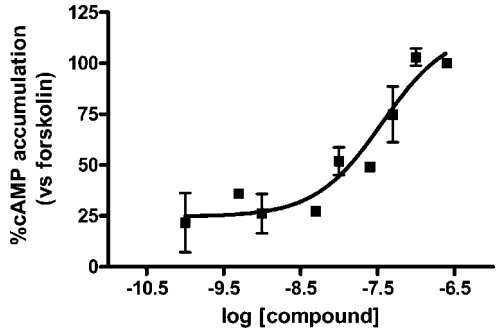

Figure 2. Effect of compound **18** on NECA-mediated cAMP accumulation (vs forskolin, set to 100%) in CHO cells stably expressing hA_3 AR. Data represent the mean ± SEM from three separate experiments. The EC_{50} value for **18** was 36.3 ± 3.1 nM.

derivatives **1**−**20** at these receptors was made to compare the A_1 and A_{2A} affinities of the new compounds with those of the corresponding 6-NO_2 TQX derivatives, which were tested at the bovine species receptors.[16,18,19,22]

It is noted that some PTP compounds show high (derivatives **7**, **12**−**14**, **16**) to good bA_1 AR affinities (compounds **9**, **11**, **15**) while they all possess low (**8**, **9**, **11**−**13**, **15**, **16**) to null (**10**, **14**, **17**, **20**) affinities for the bA_{2A} subtype, the only exception being the 4-amino-2-phenyl derivative **7** (K_i = 92.6 nM).

The 4-oxo derivatives **1**−**6** possess low or null bA_1 and bA_{2A} receptor affinity. In contrast, in the 4-amino series (derivatives **7**−**20**), several compounds displayed high bA_1 affinity and some of them also showed some affinity for the bA_{2A} receptor. The 4-amino-2-phenylpyridotriazolopyrazin-1-one derivative **7** resulted in being one of the most active at either the bA_1 (K_i = 3.1 nM) or the bA_{2A} receptor (K_i = 92.6 nM). All the substituents introduced on the 2-phenyl moiety of **7** significantly weakened the anchoring to both these receptor subtypes (compounds **8**−**11**). As expected on the basis of the SAR observed in the TQX series, insertion of the cyclohexyl and cyclopentyl rings on the 4-amino group of **7** (derivatives **12** and **13**, respectively) ameliorated the bA_1 affinity, which falls in the subnanomolar range, while it worsened the bA_{2A} binding activity. The presence of an acetyl (compound **14**) or a phenylacetyl (compound **16**) residue in R_1 maintained a high affinity for the bA_1 receptor while introduction of a benzoyl group decreased it (derivative **15**). When a second benzoyl moiety was inserted on the 4-amino group of compound **15**, the affinity for the bA_1 receptor was enhanced 2-fold (derivative **19**). As expected, all the acyl groups caused a drop in the bA_{2A} affinity (compare compounds **14**−**16**, **19** to derivative **7**), and introduction of the *p*-methoxy group on the 2-phenyl ring of the 4-amido derivatives **14** and **15** reduced both the bA_1 and bA_{2A} binding activity (compounds **17** and **18**).

Finally, it is pointed out that the replacement of the nitrobenzene moiety of the TQX series with the pyridine ring, although performed to obtain hA_3 AR antagonists, resulted in being advantageous also for the binding at the bA_1 and A_{2A} receptors. In fact, in general the PTP compounds **1**, **2**, **5**−**8**, **11**−**15**, **17**−**20** showed higher affinities at both receptors than those of the corresponding 6-NO_2 TQX derivatives[16,18,19,22] (see Table 2 in Supporting Information).

(B) Molecular Modeling Studies. Following our recently reported modeling investigations, we used our improved model of the hA_3 receptor, obtained by a rhodopsin-based homology modeling (RBHM) approach,[28−31] to recognize the hypothetical binding motif of the newly synthesized PTP derivatives. Rhodopsin-based homology modeling had been used for many years to obtain three-dimensional models of the A_3 AR, and different A_3 AR models have been published describing the hypothetical interactions with known A_3 AR ligands having different chemical scaffolds. The recently published structures of human β_2 and turkey β_1 adrenergic receptors[32,33] and, in particular, of human A_{2A} AR[34] very recently deposited provide alternative templates for GPCR modeling. However, even if the A_{2A}AR as a template for modeling other AR subtypes is under intense investigation in our laboratory, we believe that the A_{2A} AR-driven models is not sufficiently validated to replace *toutcour* the previous one. Consequently, for the appropriate comparison of our previously reported modeling studies, in particular those concerning TQX analogues, we decided to utilized the rhodopsin-based homology model in tandem with the ligand-based homology modeling (LBHM) approach used to simulate the conformational changes induced by ligand binding.[35]

The topological properties of the ligands change depending on the bulkiness of the R_1 substituents. According to the volumes, shapes, and chemical complementarities of the analyzed compounds, we obtained three different conformational models of the hA_3 receptor using the LBHM approach.[35] The volume of the transmembrane (TM) binding cavity changes from 660 Å^3 of the standard RBHM-driven model to 850 and 1000 Å^3 of the LBHM-driven models. The conventional rhodopsin-based model was used to detect the specific interaction at atomic level of this class of compounds. This model is suitable to rationalize the structure−activity relationships of compounds **1**−**11**, **14**, and **17**. The first ligand-based homology model was built by using compound **15** as reference, and the binding pocket of this model has a volume of 850 Å^3. The model was used to describe the receptor−ligand interactions of compounds **12**, **13**, **15**, **16**, and **18**. For compounds **19** and **20**, the volume of the cavity was expanded to 1000 Å^3. The most important receptor modeling perturbation, obtained by the application of the LBHM

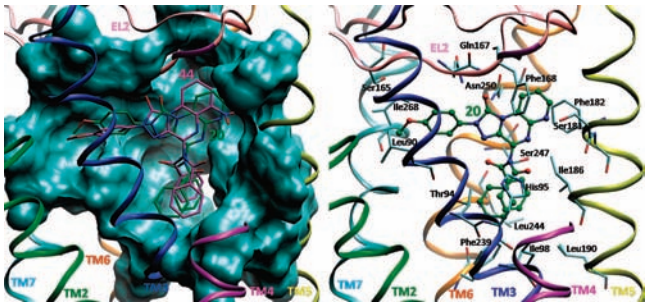

Figure 3. Left: Structure superimposition hypothetical binding motif of a representative newly synthesized pyrido[2,3-*e*]-1,2,4-triazolo[4,3-*a*]pyrazin-1-one antagonists (in green, compound **20**, K_i $hA_3AR = 7.75 \pm 0.8$) and a representative compound of 4-amido-2-aryl-1,2,4-triazolo[4,3-*a*]quinoxalin-1-ones antagonists (in magenta, compound **44**, K_i $hA_3AR = 342 \pm 21$). The most energetically favorable docked conformations of derivatives **20** and **44** are viewed from the membrane side facing TM helices 3 and 4. To clarify the TM cavity, the view of TM4 from Ser138 to Thr144 has been omitted. The surface shows the shape of the binding pocket that corresponds to residues of TMs 5, 6, and 7. Right: Hypothetical binding motif of compound **20**. Side chains of some amino acids important for ligand recognition are highlighted. Hydrogen atoms are not displayed.

technique, is the modification of both shape and volume of the hA_3 TM binding cavity, without altering the conventional rhodopsin-like receptor topology.

The binding cavity reorganization induced by ligand binding is due to the conformational change in several amino acid side chains, such as Leu90 (3.32), Leu91 (3.33), Thr94 (3.36), His95 (3.37), Ile98 (3.40), Gln167 (EL2), Phe168 (EL2), Phe182 (5.43), Ile186 (5.47), Leu190 (5.51), Phe239 (6.44), Trp243 (6.48), Leu244 (6.49), Leu264 (7.35), Ile268 (7.39). The numbering of the amino acids in parentheses follows the arbitrary scheme by Ballesteros and Weinstein:[36] according to this scheme, each amino acid identifier starts with the helix number, followed by the position relative to a reference residue among the most conserved amino acid in that helix. The reference residue is arbitrarily assigned the number 50.[36]

From the docking simulation analysis it resulted that all the PTP derivatives share a similar binding pose in the TM region of the hA_3 adenosine receptor. As shown in Figure 3, ligand recognition occurs in the upper region of the TM bundle and the PTP scaffold is surrounded by the TMs 3, 5, 6, 7 with the 1-carbonyl group pointing toward the EL2 and the substituent in the 4-position oriented toward the intracellular environment. The phenyl ring at the 2-position is close to TMs 3, 6, and 7. As observed for the TQX derivatives, the PTP antagonists present a $\pi-\pi$ stacking interaction with both side chains of Phe168 (EL2) and Phe182 (5.43) and a hydrogen bonding network in the most energetically stable docked conformations. The first hydrogen bond is between the 1-carbonyl group and the NH of the Glu167 (EL2) and Phe168 (EL2) amidic bond. A second important hydrogen bond involves the side chains of Thr94 (3.36), His95 (3.37), and Ser247 (6.52) that interact with the 4-carbonyl oxygen of compounds **1**−**6**, the 4-amino group of compounds **7**−**13**, or the 4-acylamino group of compounds **14**−**20**. This region seems to be critical both for the recognition of all antagonist structures and for receptor selectivity. In particular, Ser247 (6.52) of hA_3 receptor subtype is not present in the corresponding position of A_1 and A_2 receptors, where this amino acid is replaced by histidine (His251 in hA_1, His250 in hA_{2A}, and His251 in hA_{2B}). The histidine side chain is bulkier than serine, and probably for this reason large substituents at the 4-position of PTP framework are not well tolerated by hA_1 and hA_{2A} receptor subtypes. On the contrary, the hydroxyl group of Ser247 (6.52) of hA_3 receptor is appropriately positioned to form a hydrogen bonding interaction with the carbonyl oxygen of the 4-amido group of compounds **14**−**20**. These observations support the importance of a *N*-acyl group in modulating receptor selectivity. Specifically with reference to 4-N-acylated derivatives, the hA_3 receptor affinity increases with the bulkiness of the R_1 substituent (compare the 4-amino compounds **7** and **8** to the 4-acetylamino derivatives **14** and **17** and to the 4-benzoylamino compounds **15** and **18**).

The hydrophobic environment of the five nonpolar amino acids, Ile98 (3.40), Ile186 (5.47), Leu190 (5.51), Phe239 (6.43), and Leu244 (6.49), can justify this trend of affinity. To support this theory, hydrophobic substituents were introduced on 4-amino derivatives: cyclohexyl (compound **12**) and cyclopentyl (compound **13**) interact with this hydrophobic pocket increasing the hA_3 receptor affinity (compare compounds **12** and **13** to the unsubstituted 4-amino derivatives **7**).

Finally, as shown in Figure 3 by the comparison of the best docking poses of both the pyrido[2,3-*e*]-1,2,4-triazolo[4,3-*a*]pyrazin-1-one (in green, compound **20**, K_i $hA_3 = 7.75 \pm 0.8$ nM) and the 4-amido-6-nitro-2-phenyl-1,2,4-triazolo[4,3-*a*]quinoxalin-1-one antagonists (in magenta, compound **44**, K_i $hA_3 = 342 \pm 21$ nM), the described hydrogen bond interaction between the 6-nitro group of **44** with the side chain of Ser181 (5.42) is now replaced by the interaction with the same amino acid side chain and the endocyclic nitrogen atom of **20**.

Considering the substituent on the 2-phenyl ring, the methoxy group turned out advantageous in all the PTP derivatives, either 4-oxo, 4-amino, or 4-amido substituted. The 2-(4-methoxyphenyl) derivatives **2**, **8**, **17**, **18**, and **20** possess higher hA_3 AR affinities than the corresponding 2-phenyl derivatives **1**, **7**, **14**, **15**, and **19** because the methoxy substituent can favorably interact with Ser165 (EL2). The hydroxyl group of Ser165 is separated by 2 Å from the *p*-methoxy group and correctly oriented to form a weak hydrogen bond. The side chains of Leu90 (3.32) and Ile268 (7.39) delimit a small hydrophobic pocket that can accommodate the methoxy substituent but create unfavorable steric and dipolar interaction with the other groups (OH, F, COOH/COOEt) introduced on the 2-phenyl ring (derivatives **3**−**6**, **9**−**11**). Compounds **5** and **11** present a hydroxyl group that loses the hydrophobic interactions with Leu90 (3.32) and Ile268 (7.39) and decreases the hA_3AR affinity. The bulkiness of the carboxy acid/ester groups of compounds **4**, **6**, **10** determines the lack of affinity of these derivatives. The fluorine atom seems to have no effect because the 2-(4-fluorophenyl) derivatives **3** and **9** display comparable affinities to those of the 2-phenyl compounds **1** and **7**. The fluorine atom could interact as hydrogen bond acceptor, but in the most energetically stable conformations of compounds **3** and **9**, the distance between the fluorine and the hydroxy group of Ser165 (EL2) is more than 3 Å.

In summary, as stated above, the nitrobenzene moiety of the triazoloquinoxaline-1-one derivatives can be conveniently replaced by the pyridine ring to afford a new class of AR antagonists, the pyrido[2,3-*e*]-1,2,4-triazolo[4,3-*a*]pyrazin-1-one derivatives. The steric clashes created by the nitrobenzene with the backbone of TM5, and in particular with the peptide bond of Ser181 (5.42) and Phe182 (5.43), have been overcome, while the electrostatic effect is conserved. Moreover, the endocyclic nitrogen atom can favorably interact with the side chain of Ser181 (5.42) through a hydrogen-bond interaction. This structural modification turned out particularly beneficial in the 4-amino series **B** when the volume of the molecule is increased

by the presence of cycloalkyl and acyl substituents on the 4-amino group. Indeed, the hA_3 affinities of the PTP derivatives **12**−**15**, **17**−**20** are significantly higher than those of the corresponding TQX **39**−**46**,[16,18,19,22] with the only exception being the 4-benzoylamino derivative **15** that shows a 3-fold reduced A_3 receptor affinity compared to the triazoloquinoxaline analogue **42** (Table 2).

(C) Electrophysiological Studies. Compound **18** was investigated for its effect on synaptic transmission during severe oxygen glucose deprivation (OGD) in the CA1 region of rat hippocampal slices. In agreement with our previous results,[11,13,12,24] a direct current (dc) shift, that is, an electrophysiological signature of anoxic depolarization (AD), was always present when we applied an OGD episode of 7 min ($n = 8$, Figure 4). AD consists in a drop of neuron and glia membrane potential and represents an unequivocal sign of neuronal injury during ischemia both in vivo and in vitro.[37] The dc shift presented a mean latency of 6.6 ± 0.1 min (calculated from the beginning of OGD) and a mean peak amplitude of 7.9 ± 0.5 mV ($n = 8$) (Figure 4A). In addition, 7-min OGD completely abolished the field excitatory postsinaptic potentials (fEPSPs) which did not recover their amplitude after return to oxygenated solution (Figure 4C). Compound **18** (10 nM, $n = 8$) was checked for its effects on 7 min OGD. Figure 4B,C shows that derivative **18** prevented AD in seven out of the eight slices and delayed it in the remaining slice (Figure 4B). Moreover, it induced a significant fEPSP recovery of 77.6 ± 10.4%, ($n = 8$, $p < 0.001$, one-way ANOVA, Newman−Keuls multiple-comparison post hoc test) when compared to that found in untreated OGD slices (2.3 ± 2.0%, $n = 8$).

It is mentioned that fEPSP reduction in the CA1 hippocampus during OGD is most likely due to a reduction of glutamate release due to activation of presynaptic A_1 receptors induced by extracellular adenosine. This effect is detectable by the first 2 min of ischemia.[38] At the concentration used in our experiments, the A_1 antagonistic effect of compound **18** did not appear, since the compound did not modify the depression of fEPSP induced by OGD (Figure 4C).

In order to better characterize the effects of the A_3 antagonist on AD development, we prolonged the duration of ischemic insult from 7 to 30 min, an OGD time duration invariably harmful for the tissue.[11,39] As illustrated in Figure 4D, 30 min of OGD elicited the appearance of AD in all experimental groups. When OGD was applied in the presence of different concentrations of compound **18**, the latency of AD was always delayed (Figure 4B). A statistically significant difference from control was reached at the concentration of 10 nM (from 6.8 ± 0.1 min, $n = 15$, in the absence to 8.9 ± 0.8, $n = 5$, $P < 0.01$, in the presence of 10 nM compound **18**).

The effects of derivative **18**, on both fEPSPs and the AD delay, are similar to those previously obtained[11−13,24] with other structurally diverse compounds which proved to be effective at nanomolar concentrations in the same rat model. It is pointed out that all the previously tested derivatives[11−13,24] possessed nanomolar affinities for the hA_3 receptor but most of them showed a very low affinity for the rA_3 receptor. The discrepancy between the potency demonstrated in the rat hippocampus experiments and the rA_3 binding affinity is much more striking for compound **18**, since it shows no affinity for the cloned rA_3 receptor. We might hypothesize that the specific conformation assumed by A_3 receptors in CA1 hippocampal slices during ischemia may differ from that assessed in receptor binding experiments on disrupted HEK cell membranes. Alternatively, there could be another mechanism responsible for the electrophysiological effects of **18**. Since it is a very lipophilic compound, it might affect AD development and recovery of fEPSP by acting at an intracellular molecular target.

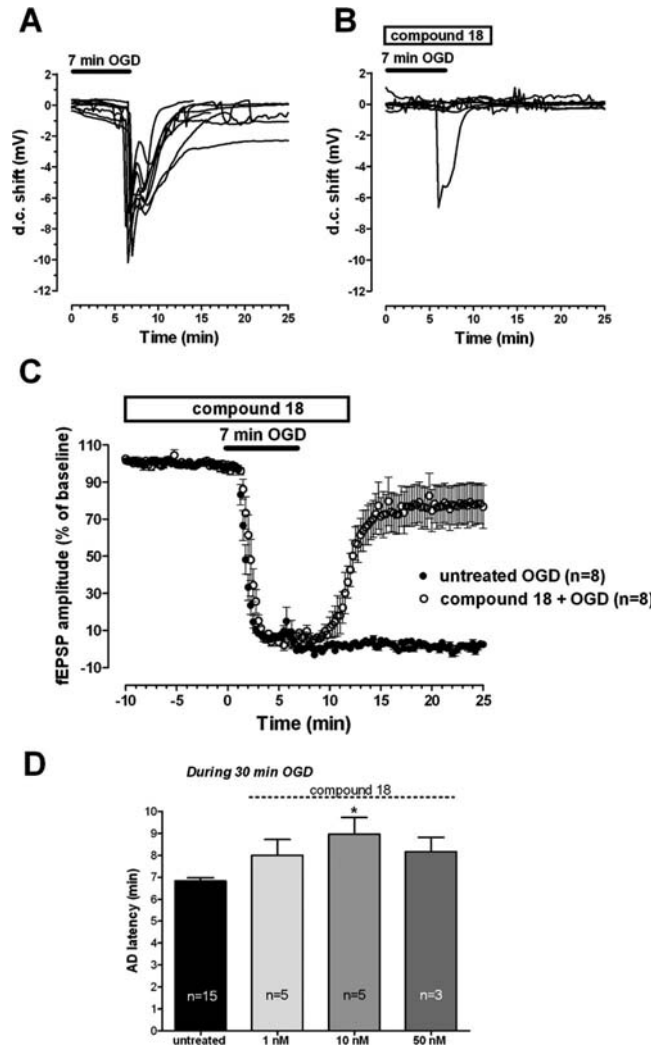

Figure 4. Compound **18** blocks or delays the appearance of AD induced by OGD and prevents the irreversible loss of neurotransmission induced by 7 min OGD in CA1 rat hippocampus. AD was recorded as the negative dc shift in response to 7 min OGD (solid bar) in the absence (A) ($n = 8$) and in the presence (B) ($n = 8$) of 10 nM compound **18** (open bar). (C) Graph shows the time course of 7 min OGD effects on fepsp amplitude in untreated (black circles, mean ± SEM, $n = 8$) OGD slices and in 10 nM compound **18** (open circles, mean ± SEM, $n = 8$) treated OGD slices. fEPSP amplitude is expressed as percent of baseline. Note that after reperfusion in oxygenated solution, a significant recovery of fEPSP was found only in treated OGD slices. (D) Each column represents the mean ± SEM of AD latency recorded in hippocampal slices during 30 min of OGD and measured from the beginning of ischemic insult. Note also that compound **18** significantly postpones AD development when used at a concentration of 10 nM: (*) $p < 0.01$, unpaired two-tailed Student's t test in comparison to untreated OGD slices. The number (n) of slices tested is reported inside columns.

In any case, compound **18** delays the occurrence of AD, brought about by a severe OGD in the CA1 region of rat hippocampal slices, and induces a significant recovery of an otherwise disrupted neurotransmission. Since AD is an unequivocal sign of brain damage during ischemia,[38] compounds that delay the AD initiation or propagation may be developed as neuroprotective agents in brain ischemia. The availability of drugs able to counteract stroke-induced neurodegeneration is an as yet unmet need.

(D) Conclusion. The present study has led to the identification of the pyrido[2,3-e]-1,2,4-triazolo[4,3-*a*]pyrazin-1-one tricyclic system as a new scaffold to obtain potent and selective hA_3 AR antagonists. In fact, some of the newly synthesized derivatives showed high hA_3 AR affinities (K_i < 50 nM) and selectivities vs both hA_1 and hA_{2A} receptors. Our recently described ligand-based homology model of the hA_3 receptor has permitted depiction of the hypothetical binding mode of the new derivatives and to rationalize the observed structure−affinity relationships. The selected 4-benzoylamino-2-(4-methoxyphenyl)pyrido[2,3-*e*]-1,2,4-triazolo[4,3-*a*]pyrazin-1-one (**18**), tested in an in vitro rat model of cerebral ischemia, proved to be effective in preventing the failure of synaptic activity induced by 7 min of OGD and delayed the occurrence of AD caused by a prolonged (30 min) OGD.

Experimental Section

(A) Chemistry. Silica gel plates (Merck F_{254}) and silica gel 60 (Merck, 70−230 mesh) were used for analytical and column chromatography, respectively. All melting points were determined on a Gallenkamp melting point apparatus. Microanalyses were performed with a Perkin-Elmer 260 elemental analyzer for C, H, N, and the results were within ±0.4% of the theoretical values unless otherwise stated. The IR spectra were recorded with a Perkin-Elmer Spectrum RX I spectrometer in Nujol mulls and are expressed in cm^{-1}. The ^1H NMR spectra were obtained with a Brucker Avance 400 MHz instrument. The chemical shifts are reported in δ (ppm) and are relative to the central peak of the solvent which was DMSO-d_6 or $CDCl_3$. The following abbreviations are used: s = singlet, d = doublet, dd = double doublet, t = triplet, m = multiplet, br = broad, ar = aromatic protons, al = aliphatic protons.

General Procedure for the Synthesis of 2-Arylhydrazono-1,2-dihydropyrido[2,3-*b*]pyrazin-3(4*H*)-ones 25−28. Ethyl N^1-arylhydrazono-N^2-chloroacetates **21**−**24**[25−27] (11 mmol) were reacted with 1,2-diamminopyridine (9.2 mmol) in refluxing ethanol (50 mL) and triethylamine (1.5 mL) for 3−4 h. The suspension was cooled at room temperature, and the solid was collected by filtration and washed with water and then with diethyl ether.

25: yield 80%; mp >300 °C (DMF); ^1H NMR 6.65−6.78 (m, ar), 6.91−7.06 (m, ar), 7.21−7.29 (m, ar), 7.55 (d, ar, J = 8.4 Hz), 7.65 (d, ar, J = 7.8 Hz), 7.78 (d, H-7, J = 4.8 Hz), 7.89 (s, NH), 8.12 (d, H-9, J = 3.9 Hz), 9.65 (s, NH), 9.74 (br s, NH), 10.97 (s, NH), 11.38 (s, NH), 12.6 (s, NH). Anal. ($C_{13}H_{11}N_5O$) C, H, N.

26: yield 68%; mp 273−275 °C (DMF); ^1H NMR 3.65 (s, CH_3), 3.69 (s, CH_3), 6.81 (d, ar, J = 8.8 Hz), 6.84−6.97 (m, ar), 7.10 (d, ar, J = 8.8 Hz), 7.51−7.53 (m, ar + NH), 7.63 (d, ar, J = 6.7 Hz), 7.75 (d, H-7, J = 3.5 Hz), 8.13 (d, H-7, J = 3.5 Hz), 9.61 (s, NH), 9.84 (s, NH), 11.16 (s, NH), 11.29 (s, NH), 12.66 (s, NH). Anal. ($C_{14}H_{13}N_5O_2$) C, H, N.

27: yield 96%; mp 288−289 °C (DMF); ^1H NMR 6.77−6.79 (m, ar), 6.99−7.17 (m, ar), 7.51 (d, ar, J = 7.8 Hz), 7.65 (d, ar, J = 7.7 Hz), 7.79 (d, H-7, J = 4.3 Hz), 7.85 (s, NH), 8.15 (d, H-7, J = 3.9 Hz), 9.59 (s, NH), 9.94−9.96 (m, NH), 10.96−11.16 (m, NH), 11.35 (br s, NH), 12.67 (br s NH). Anal. ($C_{13}H_{10}FN_5O$) C, H, N.

28: yield 85%; mp 273−275 °C (2-methoxyethanol); ^1H NMR 1.20−1.34 (m, CH_3), 4.20−4.38 (m, CH_2), 6.72−6.85 (m, ar), 6.99−7.18 (m, ar), 7.23 (d, ar, J = 8.6 Hz), 7.56−7.82 (m, ar), 7.83 (d, ar, J = 9.4 Hz), 8.16 (d, H-7, J = 4.7 Hz), 8.67 (s, NH), 9.79 (s, NH), 10.33 (s, NH), 10.71 (s, NH), 11.46 (s, NH), 11.53 (s, NH), 12.74 (s, NH). Anal. ($C_{16}H_{15}N_5O_3$) C, H, N.

General Procedure for the Synthesis of 2-Aryl-1,2-dihydropyrido[2,3-*e*]-1,2,4-triazolo[4,3-*a*]pyrazin-1,4(2*H*,5*H*)-diones 1−4. Derivatives **25**−**28** (4 mmol) were reacted with triphosgene (4 mmol, with **25** and **26**; 12 and 8 mmol with **27** and **28**, respectively) in refluxing anhydrous tetrahydrofuran (50 mL) until the disappearance (TLC monitoring) of the starting hydrazones (8−20 h). The suspension, cooled at room temperature, was diluted with water (about 50 mL) and the solid was collected by filtration.

1: yield 80%; mp >300 °C (AcOH); ^1H NMR 7.33−7.40 (m, 2H, 1 ar + H-8), 7.56−7.60 (t, 2H, ar), 8.01 (d, 2H, ar, J = 8.6 Hz), 8.34 (d, 1H, H-7, J = 4.0 Hz), 8.84 (d, 1H, H-9, J = 8.1 Hz), 12.45 (br s, 1H, NH). Anal. ($C_{14}H_9N_5O_2$) C, H, N.

2: yield 65%; mp >300 °C (DMF); ^1H NMR 3.82 (s, 3H, CH_3), 8.13 (d, 2H, ar, J = 9.1 Hz), 7.34 (dd, 1H, H-8, J = 8.1 and 4.8 Hz), 7.87 (d, 2H, ar, J = 9.1 Hz), 8.33 (d, 1H, H-7, J = 4.8 Hz), 8.83 (d, 1H, H-9, J = 8.1 Hz), 12.41 (s, 1H, NH). Anal. ($C_{15}H_{11}N_5O_3$) C, H, N.

3: yield 40%; mp >300 °C (AcOH); ^1H NMR 7.35 (dd, 1H, H-8, J = 8.0 and 4.8 Hz), 7.41−7.45 (m, 2H, ar), 8.00−8.04 (m, 2H, ar), 8.34 (d, 1H, H-7, J = 4.8 Hz), 8.83 (d, 1H, H-9, J = 8.0 Hz), 12.47 (br s, 1H, NH); IR 3414, 1728, 1705. Anal. ($C_{14}H_8FN_5O_2$) C, H, N.

4: yield 45%; mp >300 °C (DMF); ^1H NMR 1.35 (t, 3H, CH_3, J = 7.1 Hz), 4.35 (q, 2H, CH_2, J = 7.1 Hz), 7.36 (dd, 1H, H-8, J = 8.1 and 4.8 Hz), 8.16 (d, 2H, ar, J = 8.8 Hz), 8.21 (d, 2H, ar, J = 8.8 Hz), 8.35 (d, 1H, H-7, J = 4.8 Hz), 8.83 (d, 1H, H-9, J= 8.1 Hz), 12.52 (br s, 1H, NH); IR 3402, 1722, 1708, 1693. Anal. ($C_{17}H_{13}N_5O_4$) C, H, N.

2-(4-Hydroxyphenyl)-1,2-dihydropyrido[2,3-*e*]-1,2,4-triazolo[4,3-*a*]pyrazin-1,4(2*H*,5*H*)-dione 5. A BBr_3 methylene chloride solution (1 M, 5.8 mL) was dropwise added at 0 °C to a suspension of compound **2** (0.97 mmol) in anhydrous methylene chloride (15 mL) under nitrogen atmosphere. The suspension was stirred at room temperature for 5 days, then diluted with water (4 mL) and the mixture neutralized with 1 M NaOH solution. The solid was collected by filtration and washed with water. Yield 90%; mp >300 °C (DMF); ^1H NMR 6.92 (d, 2H, ar, J = 8.9 Hz), 7.33 (dd, 1H, H-8, J = 8.1 and 4.8 Hz), 7.72 (d, 2H, ar, J = 8.9 Hz), 8.32 (d, 1H, H-7, J = 4.8 Hz), 8.83 (d, 1H, H-9, J = 8.1 Hz), 9.76 (s, 1H, OH), 12.40 (s, 1H, NH); IR 3420, 3370, 1712, 1688. Anal. ($C_{14}H_9N_5O_3$) C, H, N.

2-(4-Carboxyphenyl)-1,2-dihydropyrido[2,3-*e*]-1,2,4-triazolo[4,3-*a*]pyrazin-1,4(2*H*,5*H*)-dione 6. A suspension of the ester **4** (0.85 mmol) in ethanol (20 mL) and 0.8 M NaOH aqueous solution (20 mL) was stirred at room temperature for 24 h, then acidified with 6 N HCl. The solid was collected by filtration and washed with water. Yield 75%; mp >300 °C (DMF); ^1H NMR 7.36 (dd, 1H, H-8, J = 8.1 and 4.8 Hz), 8.13 (d, 2H, ar, J = 8.8 Hz), 8.18 (d, 2H, ar, J = 8.8 Hz), 8.35 (d, 1H, H-7, J = 4.8 Hz), 8.83 (d, 1H, H-9, J= 8.1 Hz), 12.50 (br s, 1H, NH), 13.07 (br s, 1H, OH); IR 3395, 1723, 1695. Anal. ($C_{15}H_9N_5O_4$) C, H, N.

General Procedure for the Synthesis of 2-Aryl-4-chloro-1,2-dihydropyrido[2,3-*e*]-1,2,4-triazolo[4,3-*a*]pyrazin-1(2*H*)-ones 29−32. A mixture of compounds **1**−**4** (4 mmol), phosphorus penthachloride (4 mmol), phosphorus oxychloride (40 mL), and anhydrous pyridine (0.3 mL) was refluxed until the disappearance (TLC monitoring) of the starting material (2−18 h). Evaporation of the excess of phosphorus oxychloride at reduced pressure gave a residue that was treated with ice−water (50 mL). The solid was filtered, washed with water, and dried. The 4-chloro derivatives, obtained in high overall yields (75−90%) were unstable upon recrystallization; however, they were pure enough to be used without further purification.

29: ^1H NMR 7.40 (t, 1H, ar, J= 6.7 Hz), 7.52−7.59 (m, 2H, ar), 7.76 (dd, 1H, H-8, J = 8.1 and 4.4 Hz), 8.01 (d, 2H, ar, J = 8.0 Hz), 8.73 (d, 1H, H-7, J = 4.4 Hz), 9.05 (s, 1H, H-9, J = 8.1 Hz).

30: ^1H NMR 3.81 (s, 3H, Me), 7.14 (d, 2H, ar, J = 9.1 Hz), 7.77 (dd, 1H, H-8, J = 8.1 and 4.4 Hz), 7.89 (d, 2H, ar, J = 9.1 Hz), 8.73 (d, 1H, H-7, J = 4.4 Hz), 9.05 (d, 1H, H-9, J = 8.1 Hz).

31: ^1H NMR 7.44−7.48 (m, 2H, ar), 7.79 (dd, 1H, H-8, J = 8.0 and 4.8 Hz), 8.04−8.08 (m, 2H, ar), 8.76 (d, 1H, H-7, J = 4.8 Hz), 9.06 (d, 1H, H-9, J = 8.0 Hz).

32: ^1H NMR 1.36 (t, 3H, CH_3, J = 7.1 Hz), 4.36 (q, 2H, CH_2, J = 7.1 Hz),7.81 (dd, 1H, H-8, J = 8.2 and 4.7 Hz), 8.12−8.15 (m, 4H, ar), 8.76 (d, 1H, H-7, J = 4.7 Hz), 9.05 (d, 1H, H-9, J = 8.2 Hz).

General Procedure for the Synthesis of 4-Amino-2-aryl-1,2-dihydropyrido[2,3-*e*]-1,2,4-triazolo[4,3-*a*]pyrazin-1(2*H*)-ones 7−10. A suspension of the 4-chloro derivatives **29**−**32** (2 mmol), in absolute ethanol (30 mL) saturated with ammonia, was heated overnight at 120 °C in a sealed tube. After the mixture was cooled at room temperature, the solid was collected by filtration and washed with water.

7: yield 75%; mp >300 °C (AcOH); ^{1}H NMR 7.25−7.40 (m, 4H, ar), 7.56 (t, 2H, ar, J = 7.7 Hz), 7.90−8.06 (m, 4H, 2ar + NH_2), 8.42 (d, 1H, H-7, J = 4.8 Hz), 8.85 (d, 1H, H-9, J = 8.1 Hz); IR 3420, 3240, 1700. Anal. ($C_{14}H_{10}N_6O$) C, H, N.

8: yield 70%; mp >300 °C (AcOH); ^{1}H NMR 3.82 (s, 3H, CH_3), 7.13 (d, 2H, ar, J = 9.1 Hz), 7.27 (dd, 1H, H-8, J = 8.0 and 4.8 Hz), 7.89−8.05 (m, 4H, 2ar + NH_2), 8.43 (d, 1H, H-7, J = 4.8 Hz), 8.85 (d, 1H, H-9, J = 8.0 Hz); IR 3428, 3230, 1710. Anal. ($C_{15}H_{12}N_6O_2$) C, H, N.

9: yield 95%; mp >300 °C (2-methoxyethanol); ^{1}H NMR 7.28 (dd, 1H, H-8, J = 8.0 and 4.8 Hz), 7.44 (t, 2H, J = 8.8 Hz), 7.80−8.08 (m, 4H, 2ar + NH_2), 8.44 (d, 1H, H-7, J = 4.8 Hz), 8.85 (d, 1H, H-9, J = 8.0 Hz); IR 3482, 1715. Anal. ($C_{14}H_9FN_6O$) C, H, N.

10: yield 64%; mp >300 °C (DMF); ^{1}H NMR 1.36 (t, 3H, CH_3, J = 7.1 Hz), 4.36 (q, 2H, CH_2, J = 7.1 Hz), 7.29 (dd, 1H, H-8, J = 8.0 and 4.8 Hz), 8.01 (br s, 2H, NH_2), 8.16 (d, 2H, ar, J = 8.7 Hz), 8.26 (d, 2H, ar, J = 8.7 Hz), 8.45 (d, 1H, H-7, J = 4.8 Hz), 8.85 (d, 1H, H-9, J = 8.0 Hz); IR 3380, 1727, 1715. Anal. ($C_{17}H_{14}N_6O_3$) C, H, N.

4-Amino-2-(4-hydroxyphenyl)-1,2-dihydropyrido[2,3-*e*]-1,2,4-triazolo[4,3-*a*]pyrazin-1(2*H*)-one 11. A BBr_3 methylene chloride solution (1M, 5.8 mL) was dropwise added at 0 °C to a suspension of compound **8** (0.97 mmol) in anhydrous methylene chloride (15 mL) under nitrogen atmosphere. The suspension was stirred at room temperature for 4 days, then diluted with water (4 mL) and the mixture neutralized with 1 M NaOH solution. The solid was collected by filtration and washed with water. Yield 95%; mp >300 °C (DMF); ^{1}H NMR 6.92 (d, 2H, ar, J = 8.9 Hz), 7.26 (dd, 1H, H-8, J = 8.0 and 4.7 Hz), 7.75 (d, 2H, ar, J = 8.9 Hz), 7.80 (br s, 2H, NH_2), 8.43 (d, 1H, H-7, J = 4.7 Hz), 8.85 (d, 1H, H-9, J = 8.0 Hz), 9.77 (s, 1H, OH); IR 3440, 3315, 1720. Anal. ($C_{14}H_{10}N_6O_2$) C, H, N.

4-Cyclohexylamino-2-phenyl-1,2-dihydropyrido[2,3-*e*]-1,2,4-triazolo[4,3-*a*]pyrazin-1(2*H*)-one 12. A mixture of the 4-chloro derivative **29** (1 mmol) and cyclohexylamine (1.2 mmol) in absolute ethanol (5 mL) was heated overnight at 120 °C in a sealed tube. After the mixture was cooled at room temperature, the solid was collected by filtration and washed with water. Yield 78%; mp 199−200 °C (cyclohexane); ^{1}H NMR 1.18−2.0 (m, 10H, al), 4.10−4.25 (m, 1H, al), 7.20−7.39 (m, 2H, ar + H-8), 7.57 (t, 2H, ar, J = 7.2 Hz), 8.06 (d, 2H, ar, J = 7.2 Hz), 8.19 (d, 1H, NH, J = 8.7 Hz), 8.41 (d, 1H, H-7, J = 3.7 Hz), 8.85(d, 1H, H-9, J = 6.6 Hz); IR 3500, 3370, 1700. Anal. ($C_{20}H_{20}N_6O$) C, H, N.

4-Cyclopentylamino-2-phenyl-1,2-dihydropyrido[2,3-*e*]-1,2,4-triazolo[4,3-*a*]pyrazin-1(2*H*)-one 13. The title compound was prepared by reacting derivative **29** (1.0 mmol) and cyclopentylamine (1.2 mmol) in the conditions described above to prepare compound **12**. Yield 75%; mp 190−191 °C (cyclohexane/EtOAc); ^{1}H NMR 1.5−2.5 (m, 8H, al), 4.42−4.65 (m, 1H, al), 7.21−7.39 (m, 2H, ar + H-8), 7.57 (t, 2H, ar, J = 7.3 Hz), 8.06 (d, 2H, ar, J = 7.3 Hz), 8.29 (d, 1H, NH, J = 7.7 Hz), 8.41 (d, 1H, H-7, J = 4.7 Hz), 8.84 (d, 1H, H-9, J = 8.0 Hz); IR 3290, 1730. Anal. ($C_{19}H_{18}N_6O$) C, H, N.

General Procedure for the Synthesis of 4-Amido-2-aryl-1,2-dihydropyrido[2,3-*e*]-1,2,4-triazolo[4,3-*a*]pyrazin-1(2*H*)-ones 14−18. A mixture of the 4-amino derivative **7** or **8** (1.1 mmol) and acetyl chloride (1.2 mmol), benzoyl chloride (1.7 mmol), or phenylacetyl chloride (3.2 mmol) in anhydrous pyridine (10 mL) was refluxed until the disappearance (TLC monitoring) of the starting 4-amino derivative (2−5 h). After cooling at room temperature, the suspension was diluted with water (30 mL) and the solid was collected and washed with water.

14: yield 70%; mp >300 °C (DMF); ^{1}H NMR 2.46 (s, 3H, CH_3), 7.40 (t, 1H, ar, J = 7.3 Hz), 7.57−7.61 (m, 3H, 2ar + H-7), 8.11 (d, 2H, ar, J = 8.0 Hz), 8.63 (d, 1H, H-7, J = 4.8 Hz), 8.99 (d, 1H, H-9, J = 8.1 Hz), 10.72 (br s, 1H, NH); IR 1715, 1695. Anal. ($C_{16}H_{12}N_6O_2$) C, H, N.

15: yield 84%; mp 244−246 °C (2-methoxyethanol); ^{1}H NMR 7.38 (t, 1H, ar, J = 7.4 Hz), 7.55−7.69 (m, 6H, ar), 7.99 (d, 2H, ar, J = 7.6 Hz), 8.03−8.13 (m, 2H, ar), 8.57 (br s, 1H, ar), 8.98 (br s, 1H, H-9), 11.45 (br s, 1H, NH); IR 1719, 1654. Anal. ($C_{21}H_{14}N_6O_2$) C, H, N.

16: yield 35%; mp 240−241 °C (acetonitrile); ^{1}H NMR 4.11 (s, 2H, CH_2), 7.28−7.43 (m, 6H, ar), 7.58−7.62 (m, 3H, ar), 8.09 (d, 2H, ar, J = 7.7 Hz), 8.64 (d, 1H, H-7, J = 4.7 Hz), 8.99 (d, 1H, H-9, J = 8.1 Hz), 10.95 (s, 1H, NH); IR 3340−3430, 1727, 1688. Anal. ($C_{22}H_{16}N_6O_2$) C, H, N.

17: yield 55%; mp 278−280 °C (2-ethoxyethanol); ^{1}H NMR 2.42 (s, 3H, $COCH_3$), 3.83 (s, 3H, OCH_3), 7.14 (d, 2H, ar, J = 9.0 Hz), 7.57 (dd, 1H, H-8, J = 7.9 and 4.5 Hz), 7.96 (d, 2H, ar, J = 9.0 Hz), 8.63 (d, 1H, H-7, J = 4.5 Hz), 8.98 (d, 1H, H-9, J = 7.9 Hz), 10.73 (br s, 1H, NH); IR 3485−3358 1716, 1691. Anal. ($C_{17}H_{14}N_6O_3$) C, H, N.

18: yield 88%; mp 250−252 °C (2-ethoxyethanol); ^{1}H NMR 3.81 (s, 3H, CH_3), 7.12 (d, 2H, ar, J = 9.0 Hz), 7.55−7.69 (m, 4H, ar), 7.85 (d, 2H, ar, J = 8.3 Hz), 8.11−8.13 (m, 2H, ar), 8.52−8.56 (m, 1H, ar), 9.02 (br s, 1H, H-9), 11.42 (br s, 1H, NH); IR 1717. Anal. ($C_{22}H_{16}N_6O_3$) C, H, N.

4-Dibenzoylamino-2-phenyl-1,2-dihydropyrido[2,3-*e*]-1,2,4-triazolo[4,3-*a*]pyrazin-1(2*H*)-ones 19. A mixture of the 4-amino derivative **7** (1.8 mmol) and benzoyl chloride (16 mmol) in anhydrous pyridine was refluxed for 28 h. After cooling at room temperature, the suspension was diluted with water and the solid collected by filtration and recrystallized. Yield 60%; mp 276−278 °C (DMF); ^{1}H NMR 7.36 (t, 1H, ar, J = 7.4 Hz), 7.51−7.55 (m, 6H, ar), 7.65−7.68 (m, 2H, ar), 7.73 (dd, 1H, H-8, J = 8.2 and 4.5 Hz), 7.87 (d, 2H, ar, J = 8.0 Hz), 7.93 (d, 4H, ar, J = 7.4 Hz), 8.63 (d, 1H, H-7, J = 4.5 Hz), 9.07 (d, 1H, H-9, J = 8.2 Hz); IR 1725, 1710. Anal. ($C_{28}H_{18}N_6O_3$) C, H, N.

4-Dibenzoylamino-2-(4-methoxyphenyl)-1,2-dihydropyrido[2,3-*e*]-1,2,4-triazolo[4,3-*a*]pyrazin-1(2*H*)-ones 20. A mixture of the 4-amino derivative **8** (1.3 mmol) and benzoyl chloride (3.9 mmol) in anhydrous pyridine was refluxed for 30 h. After cooling at room temperature, the suspension was diluted with water and the solid was collected by filtration. The crude solid was a mixture of compounds **20** and **15** (about 1:1 ratio, from ^{1}H NMR spectrum) which where separated by column chromatography (eluent CH_2Cl_2/EtOAc, 7:3). Evaporation of the first eluates afforded the desired compound **20**; from the second eluates the 4-benzoylamino derivative **15** and also the 1,4-dione **2** was obtained. Yield 8%; mp 287−289 °C (2-methoxyethanol); ^{1}H NMR 3.79 (s, 3H, CH_3), 7.10 (d, 2H, ar, J = 9.1 Hz), 7.53 (t, 4H, ar, J = 7.7 Hz), 7.67 (t, 2H, ar, J= 7.7 Hz), 7.72−7.77 (m, 3H, 2ar + H-8), 7.93 (d, 4H, ar, J = 7.7 Hz), 8.63 (d, 1H, H-7, J = 4.7 Hz), 9.07 (d, 1H, H-9, J = 8.2 Hz); IR 1715, 1704. Anal. ($C_{29}H_{20}N_6O_4$) C, H, N.

(B) Computational Methodologies. All modeling studies were carried out on a 16 CPU (Intel Core 2 Quad CPU 2.40 GHz) Linux cluster. Homology modeling, energy calculation, and docking studies were performed using the Molecular Operating Environment (MOE, version 2007.09) suite.[40] All docked structures were fully optimized without geometry constraints using RHF/AM1 semiempirical calculations. Vibrational frequency analysis was used to characterize the minima stationary points (zero imaginary frequencies). The software package MOPAC (version 7),[41] implemented in MOE suite, was utilized for all quantum mechanical calculations.

Homology Model of the hA_3 AR. On the basis of the assumption that GPCRs share similar TM boundaries and overall topology, a homology model of the hA_3 receptor was constructed. First, the amino acid sequences of TM helices of the A_3 receptor were aligned with those of bovine rhodopsin,[42] guided by the highly conserved amino acid residues, including the DRY motif (Asp3.49, Arg3.50, and Tyr3.51) and three proline residues (Pro4.60, Pro6.50, and Pro7.50) in the TM segments of GPCRs. The same boundaries were

applied for the TM helices of the A_3 receptor as they were identified from the X-ray crystal structure for the corresponding sequences of bovine rhodopsin,[42] the C_R coordinates of which were used to construct the seven TM helices for the hA_3 receptor. The loop domains of the hA_3 receptor were constructed by the loop search method implemented in MOE. In particular, loops are modeled first in random order. For each loop, a contact energy function analyzes the list of candidates collected in the segment searching stage, taking into account all atoms already modeled and any atoms specified by the user as belonging to the model environment. These energies are then used to make a Boltzmann-weighted choice from the candidates, the coordinates of which are then copied to the model. Any missing side chain atoms are modeled using the same procedure. Side chains belonging to residues whose backbone coordinates were copied from a template are modeled first, followed by side chains of modeled loops. Outgaps and their side chains are modeled last. Special caution has to be given to the second extracellular loop (EL2), which has been described in bovine rhodopsin as folding back over transmembrane helices[42] and, therefore, limiting the size of the active site. Hence, amino acids of this loop could be involved in direct interactions with the ligands. A driving force to this peculiar fold of the EL2 loop might be the presence of a disulfide bridge between cysteines in TM3 and EL2. Since this covalent link is conserved in all receptors modeled in the current study, the EL2 loop was modeled using a rhodopsin-like constrained geometry around the EL2−TM3 disulfide bridge. After the heavy atoms were modeled, all hydrogen atoms were added, and the protein coordinates were then minimized with MOE using the AMBER94 force field.[43] The minimizations were carried out by the 1000 steps of steepest descent followed by conjugate gradient minimization until the rms gradient of the potential energy was less than 0.1 kcal mol^{-1} $Å^{-1}$. Protein stereochemistry evaluation was performed by several tools (Ramachandran and χ plots measure φ/ψ and $\chi1/\chi2$ angles, clash contacts reports) implemented in MOE suite.[40]

Ligand-Based Homology Modeling. We have recently revisited the rhodopsin-based model of the human A_3 receptor in its resting state (antagonist-like state), taking into account a novel strategy to simulate the possible receptor reorganization induce by the antagonist-binding.[35] We called this new strategy *ligand-based homology modeling*. Briefly, the ligand-based homology modeling technique is an evolution of a conventional homology modeling algorithm based on a Boltzmann-weighted randomized modeling procedure adapted from Levitt,[44] combined with specialized logic for the proper handling of insertions and deletions any selected atoms. The *ligand-based* option is very useful when one wishes to build a homology model in the presence of a ligand docked to the primary template, or other proteins known to be complexed with the sequence to be modeled.[40] In this specific case both model building and refinement take into account the presence of the ligand in terms of specific steric and chemical features. In order to generate an initial ensemble of ligand poses, a conventional docking procedure (see next paragraphs for details) with reduced van der Waals radii (equal to 75%) and an increased Coulomb−vdW cutoff (cutoff on 10 Å, cutoff on 12 Å) has been performed. For each pose, a homology model is then generated to accommodate the ligand by reorienting nearby side chains. These residues and the ligand are then locally minimized. Finally, each ligand is redocked into its corresponding low energy protein structures and the resulting complexes are ranked according to MOEScore.[40]

Different quantitative measures of molecular volume of the receptor binding cavities have been carried out using MOE suite.[40] Prediction of antagonist−receptor complex stability (in terms of corresponding pK_i value) and the quantitative analysis for non-bonded intermolecular interactions (H-bonds, transition metal, water bridges, hydrophobic) were calculated and visualized using several tools implemented into MOE suite.[40]

Molecular Docking of the hA_3 AR Antagonists. All antagonist structures were docked into the hypothetical TM binding site by using the MOE-Dock tool, part of the MOE suite.[40] Searching is conducted within a user-specified 3D docking box, using the Tabù Search protocol[45] and the MMFF94 force field.[46] MOE-Dock performs a user-specified number of independent docking runs (50 in our specific case) and writes the resulting conformations and their energies in a molecular database file. The resulting docked complexes were subjected to MMFF94 energy minimization until the rms of conjugate gradient was <0.1 kcal mol^{-1} $Å^{-1}$. Charges for the ligands were imported from the MOPAC output files. To better refine all antagonist−receptor complexes, a rotamer exploration of all side chains involved in the antagonist-binding was carried out. Rotamer exploration methodology was implemented in MOE suite.[40]

(C) Biochemistry. Bovine A_1 and A_{2A} Receptor Binding. Displacement of [^{3}H]DPCPX from A_1 ARs in bovine cortical membranes and [^{3}H]CGS 21680 from A_{2A} ARs in bovine striatal membranes was performed as described in refs 47 and 48, respectively.

Human A_1, A_{2A}, and A_3 Receptor Binding. Binding experiments at hA_1 and hA_{2A} ARs, stably expressed in CHO cells, were performed as previously described,[49] using [^{3}H]DPCPX and [^{3}H]N-ECA, respectively, as radioligands. Displacement of [^{125}I]AB-MECA from hA_3 AR, stably expressed in CHO cells, was performed as reported in ref 16.

Rat A_1 and A_{2A} Receptor Binding. Rat brain cortex was dissected from male Wistar rats. Membrane preparation was carried out as previously reported for the bovine membrane preparation.[48] The A_1 binding assays were performed in triplicate by incubating aliquots of brain cortex membranes (40−50 μg of protein) at 25 °C for 180 min in 0.5 mL of binding buffer (50 mM Tris-HCl, 2 mM $MgCl_2$ pH 7.7) containing 0.2−0.5 nM [^{3}H]DPCPX. Nonspecific binding was defined in the presence of 20 μM R-PIA. Incubation was terminated by rapid filtration through Whatman GF/C glass microfiber filters and washing twice with 4 mL of ice-cold buffer. The dissociation constant (K_d) of [^{3}H]DPCPX on brain cortex was 0.51 nM.[50] Binding assays at the rA_{2A} were performed as previously described.[48]

Rat A_3 Receptor Binding. Membrane preparation of rat A_3 adenosine receptor expressed in HEK-293/EBNA cells was purchased from PerkinElmer Life Sciences (Boston, MA), and the radioligand binding assay was performed following manufacturer's instructions. Briefly, aliquots of cell membranes (3.9 μg) were incubated at 25 °C for 120 min in 100 μL of buffer (50 mM Tris-HCl, 10 mM $MgCl_2$, 1 mM EDTA, 1.5 units/mL ADA, pH 7.6) in the presence of 2.1 nM [^{125}I]ABMECA. Nonspecific binding was determined in the presence of 100 μM R-PIA. The K_d value of [^{125}I]AB-MECA in rat A_3 HEK-293/EBNA cell membranes was 1.97 nM. Bound radioactivity was separated by rapid filtration through GF/C glass fiber filters presoaked in 0.5% polyethylenimine and washed nine times with 0.5 mL of ice-cold 50 mM Tris-HCl, 10 mM $MgCl_2$, 1 mM EDTA, pH 7.6. The radioactivity was measured by γ scintillation spectrometry.

Measurement of cAMP Levels on CHO Cells Transfected with Human A_{2B} and A_3 ARs. Intracellular cAMP levels were measured using a competitive protein binding method.[51] CHO cells (~60 000), stably expressing hA_{2B} or hA_3 ARs, were plated in 24-well plates. After 48 h, the medium was removed, and the cells were incubated at 37 °C for 15 min with 0.5 mL of di DMEM in the presence of Ro 20-1724 (4-(3-butoxy-4-methoxybenzyl)imidazolidin-2-one) (20 μM) and adenosine deaminase (1 U/mL). A stock 1 mM solution of the tested compound was prepared in DMSO, and subsequent dilutions were accomplished in distilled water. The antagonistic profile of the new compound toward hA_{2B} AR was evaluated assessing its ability to inhibit 100 nM NECA-mediated accumulation of cAMP. The antagonistic profile of the new compound toward hA_3 AR was evaluated by assessing its ability to counteract 100 nM NECA-mediated inhibition of cAMP accumulation stimulated by 1 μM forskolin. Cells were incubated in the reaction medium (15 min at 37 °C) with different compound concentrations (1 nM to 10 μM) and then treated with NECA.

The reaction was terminated by removing the medium and adding 0.4 N HCl. After 30 min the lysate was neutralized with 4 N KOH and the suspension was centrifuged at 800*g* for 5 min. To determine

cyclic AMP production, the binding protein, prepared from beef adrenal glands, was incubated with [^{3}H]cAMP (2 nM) in distilled water, 50 μL of cell lysate, or standard cAMP (0−16 pmol) at 4 °C for 150 min in a total volume of 300 μL. Bound radioactivity was separated by rapid filtration through GF/C glass fiber filters and washed twice with 4 mL of 50 mM Tris-HCl, pH 7.4. The radioactivity was measured by liquid scintillation spectrometry.

Data Analysis. The concentration of the tested compounds that produced 50% inhibition of specific [^{3}H]DPCPX, [^{3}H]NECA, [^{3}H]CGS 21680, and [^{125}I]AB-MECA binding (IC_{50}) was calculated using a nonlinear regression method implemented by the InPlot program (Graph-Pad, San Diego, CA) with five concentrations of displacer, each performed in triplicate. Inhibition constants (K_i) were calculated according to the Cheng−-Prusoff equation.[52] The dissociation constant (K_d) values of [^{3}H]DPCPX and [^{3}H]CGS 21680 in cortical and striatal bovine brain membranes were 0.3 and 14 nM, respectively.The K_d values of [^{3}H]DPCPX, [^{3}H]NECA, and [^{125}I]AB-MECA in hA_1, hA_{2A}, and hA_3 ARs in CHO cell membranes were 3, 30, and 1.4 nM, respectively. EC_{50} values obtained in cAMP assays were calculated by nonlinear regression analysis using the equation for a sigmoid concentration−response curve (Graph-Pad, San Diego, CA).

(D) Electrophysiological Assays. Slice Preparation. All animal procedures were conducted according to the European Community Guidelines for Animal Care, DL 116/92, application of the European Communities Council Directive (86/609/EEC). Experiments were carried out on acute hippocampal slices,[11] prepared from male Wistar rats (Harlan Italy; Udine Italy, 150−200 g body weight). Animals were killed with a guillotine under anesthesia with ether, and their hippocampi were rapidly removed and placed in ice-cold oxygenated (95% O_2 and 5% CO_2) artificial cerebrospinal fluid (aCSF) of the following composition (mM): NaCl 125, KCl 3, NaH_2PO_4 1.25, $MgSO_4$ 1, $CaCl_2$ 2, $NaHCO_3$ 25, and D-glucose 10. Slices (400 μm thick) were cut using a McIlwain tissue chopper (The Mickle Laboratory, Engineering, Co. Ltd., Gomshall, U.K.) and kept in oxygenated aCSF for at least 1 h at room temperature. A single slice was then placed on a nylon mesh, completely submerged in a small chamber (0.8 mL), and superfused with oxygenated aCSF (31−32 °C) at a constant flow rate of 1.5−1.8 mL min^{-1}. The treated solutions reached the preparation in 60 s, and this delay was taken into account in our calculations.

Extracellular Recording. Test pulses (80 μs, 0.066 Hz) were delivered through a bipolar nichrome electrode positioned in the stratum radiatum. Evoked extracellular potentials were recorded with glass microelectrodes (2−10 MΩ, Harvard Apparatus LTD, Edenbridge, U.K.) filled with 150 mM NaCl and placed in the CA1 region of the stratum radiatum. Responses were amplified (BM 622, Mangoni, Pisa, Italy), digitized (sample rate, 33.33 kHz), and stored for later analysis with LTP (version 2.30D) program.[53] Stimulus−response curves were obtained by gradual increases in stimulus strength at the beginning of each experiment, when a stable baseline of evoked response was reached. The test stimulus pulse was then adjusted to produce a field excitatory postsynaptic potential (fepsp) whose slope and amplitude was 40−50% of the maximum and was kept constant throughout the experiment. The fepsp amplitude was routinely measured and expressed as the percentage of the average amplitude of the potentials measured during the 5 min preceding exposure of the hippocampal slices to OGD. In some experiments, both the amplitude and initial fepsp slope were quantified, but because no appreciable differences between these two parameters were observed in drug effect and OGD, only the amplitude measurement is expressed in the figures. Simultaneously with fepsp amplitude, AD was recorded as negative extracellular direct current (dc) shifts induced by 7 or 30 min of OGD. The dc potential is an extracellular recording considered to provide an index of the polarization of cells surrounding the tip of the glass electrode.[54]

Application of OGD and Drugs. OGD was obtained by perfusing the slice with aCSF without glucose and gassed with nitrogen (95% N_2 and 5% CO_2).[55] This caused a drop in pO_2 in the recording chamber from ∼500 mmHg (normoxia) to a range of 35−75 mmHg (after 7 min of OGD).[56] At the end of the ischemic period, the slice was again superfused with normal, glucose-containing, oxygenated aCSF. When slices were subjected to 7 min of OGD, if the recovery of fEPSP amplitude after 15 min of reperfusion with glucose-containing and normally oxygenated aCSF was ≤15% of the preischemic value, a second slice from the same rat was submitted to a 7 min OGD insult in the presence of compound **18**. To confirm the result obtained in the treated group, a third slice was taken from the same rat and another 7 min OGD was performed in control conditions to verify that no difference between slices was caused by the time gap between the experiments. The selective A_3 adenosine receptor antagonist was applied 15 min before, during, and 5 min after OGD. The compound was made up to a 100 μM stock solution in dimethyl sulfoxide (DMSO). These stock solutions were aliquoted, stored at −20 °C, and diluted in aCSF before use. The final concentration of DMSO (0.05% and 0.01% in aCSF) used in our experiments did not affect either fepsp amplitude or the depression of synaptic potentials induced by OGD (not shown).

Statistics. Data were analyzed using Prism 3.02 software (Graphpad Software, San Diego, CA). All numerical data are expressed as the mean ± SEM. Data were tested for statistical significance with the paired two-tailed Student's *t* test or by analysis of variance (one-way ANOVA), as appropriate. When significant differences were observed, the Newman−Keuls multiple comparison test was done. A value of $p < 0.05$ was considered significant.

Acknowledgment. This work was supported by a grant of the Italian Ministry for University and Research (MIUR, FIRB RBNE03YA3L Project). The molecular modeling work coordinated by S.M. was carried out with financial support from the University of Padova, Italy, and the Italian Ministry for University and Research (MIUR), Rome, Italy. The electrophysiological work was supported by a grant from the University of Florence and by Ente Cassa di Risparmio di Firenze. We thank Dr. Karl-Norbert Klotz of the University of Wüzburg, Germany, for providing cloned hA_1, hA_{2A}, and hA_3 receptors expressed in CHO cells. S.M. is also very grateful to Chemical Computing Group for the scientific and technical partnership.

Supporting Information Available: Combustion analysis data of the newly synthesized compounds; binding affinities of some PTP derivatives and the corresponding 6-nitro-TQX compounds at bovine A_1 and A_{2A} ARs. This material is available free of charge via the Internet at http://pubs.acs.org.

References

(1) Fredholm, B. B.; IJzerman, A. P.; Jacobson, K. A.; Klotz, K. N.; Linden, J. International union of Pharmacology XXV. Nomenclature and classification of adenosine receptors. *Pharmacol. Rev.* **2001**, *53*, 527–552.

(2) Jacobson, K. A.; Knutsen, L. J. S. P1 and P2 Purine and Pyrimidine Receptor Ligands. In *Purinergic and Pyrimidinergic Signalling*; Abbracchio, M. P., Williams, M., Eds.; Handbook of Experimental Pharmacology, Vol. 151/1; Springer: Berlin, 2001; pp 129−175.

(3) Abbracchio, M. P.; Brambilla, R.; Kim, H. O.; von Lubitz, D. K. J. E.; Jacobson, K. A.; Cattabeni, F. G-Protein-dependent activation of phospholipase-C by adenosine A_3 receptor in rat brain. *Mol. Pharmacol.* **1995**, *48*, 1083–1045.

(4) Ali, H.; Choi, O. H.; Fraundorfer, P. F.; Yamada, K.; Gonzaga, H. M. S.; Beaven, M. A. Sustained activation of phospholipase-D via adenosine A_3 receptors is associated with enhancement of antigen-ionophore-induced and Ca^{2+}-ionophore-induced secretion in a rat mast-cell line. *J. Pharmacol. Exp. Ther.* **1996**, *276*, 837–845.

(5) Shneyvays, V.; Leshem, D.; Zinman, T.; Mamedova, L. K.; Jacobson, K. A.; Shainberg, A. Role of adenosine A_1 and A_3 receptors in regulation of cardiomyocyte homeostasis after mitochondrial respiratory chain injury. *Am. J. Physiol.: Heart Circ. Physiol.* **2005**, *288*, H2792–H2801.

(6) Schulte, G.; Fredholm, B. B. Signalling from adenosine receptors to mitogen-activated protein kinases. *Cell. Signal.* **2003**, *15*, 813–827.

(7) Brambilla, R.; Cattabeni, F.; Ceruti, S.; Barbieri, D.; Franceschi, C.; Kim, Y.-C; Jacobson, K. A.; Klotz, K.-N; Lohse, M. J.; Abbracchio, M. P. Activation of the A_3 adenosine receptor affect cell cycle

progression and cell growth. *Naunyn-Schmiedeberg's Arch. Pharmacol.* **2000**, *361*, 225–234.
(8) Lee, H. T.; Ota-Setlik, A.; Xu, H.; D'Agati, V. D.; Jacobson, M. A.; Emala, C. W. A_3 adenosine receptor knockout mice are protected against ischemia- and myoglobinuria-induced renal failure. *Am. J. Physiol. Renal Physiol.* **2003**, *284*, 267–273.
(9) Merighi, S.; Benini, A.; Mirandola, P.; Gessi, S.; Varani, K.; Leung, E.; Maclennan, S.; Borea, P. A. Adenosine modulates vascular endotelial growth factor expression via hypoxia-inducible factor-1 in human glioblastoma cells. *Biochem. Pharmacol.* **2006**, *72*, 19–31.
(10) Yang, H.; Avila, M. Y.; Peterson-Yantorno, K.; Coca-Prados, M.; Stone, R. A.; Jacobson, K. A.; Civan, M. M. The cross-species A_3 adenosine receptor antagonist MRS 1292 inhibits adenosine-triggered human non pigmented ciliary epithelial cell fluid release and reduces mouse intraocular pressure. *Curr. Eye Res.* **2005**, *30*, 747–754.
(11) Pugliese, A. M.; Coppi, E.; Spalluto, G.; Corradetti, R.; Pedata, F. A_3 adenosine receptor antagonists delay irreversible synaptic failure caused by oxygen and glucose deprivation in the rat CA1 hippocampus in vitro. *Br. J. Pharmacol.* **2006**, *147*, 524–532.
(12) Pugliese, A. M.; Coppi, E.; Volpini, R.; Cristalli, G.; Corradetti, R.; Jeong, L. S.; Jacobson, K. A.; Pedata, F. Role of adenosine A_3 receptors on CA1 hippocampal neurotransmission during oxygen−glucose deprivation episodes of different duration. *Biochem. Pharmacol.* **2007**, *74*, 768–779.
(13) Colotta, V.; Catarzi, D.; Varano, F.; Capelli, F.; Lenzi, O.; Filacchioni, G.; Martini, C.; Trincavelli, L.; Ciampi, O.; Pugliese, A. M.; Pedata, F.; Schiesaro, A.; Morizzo, E.; Moro, S. New 2-arylpyrazolo[3,4-*c*]quinoline derivatives as potent and selective human A_3 adenosine receptor antagonists: synthesis, pharmacological evaluation, and ligand−receptor modeling studies. *J. Med. Chem.* **2007**, *50*, 4061–4074.
(14) Pedata, F.; Pugliese, A. M.; Coppi, E.; Popoli, P.; Morelli, M.; Schwarzschild, M. A.; Melani, A. Adenosine in the central nervous system: effects on neurotransmission and neuroprotection. *Immunol., Endocr. Metab. Agents Med. Chem.* **2007**, *7*, 304–321.
(15) Colotta, V.; Catarzi, D.; Varano, F.; Cecchi, L.; Filacchioni, G.; Martini, C.; Trincavelli, L.; Lucacchini, A. 1,2,4-Triazolo[4,3-*a*]quinoxalin-1-one: a versatile tool for the synthesis of potent and selective adenosine receptor antagonists. *J. Med. Chem.* **2000**, *43*, 1158–1164.
(16) Colotta, V.; Catarzi, D.; Varano, F; Filacchioni, G.; Martini, C.; Trincavelli, L.; Lucacchini, A. Synthesis and structure−activity relationships of a new set of 1,2,4-triazolo[4,3-*a*]quinoxalin-1-one derivatives as adenosine receptor antagonists. *Bioorg. Med. Chem.* **2003**, *11*, 3541–3550.
(17) Colotta, V.; Catarzi, D.; Varano, F; Filacchioni, G.; Martini, C.; Trincavelli, L.; Lucacchini, A. Synthesis of 4-amino-6-(hetero)arylalkylamino-1,2,4-triazolo[4,3-*a*]quinoxalin-1-one derivatives as potent A_{2A} adenosine receptor antagonists. *Bioorg. Med. Chem.* **2003**, *11*, 5509–5518.
(18) Colotta, V.; Catarzi, D.; Varano, F; Filacchioni, G.; Martini, C.; Trincavelli, L.; Lucacchini, A. Synthesis and structure−activity relationships of 4-cycloalkylamino-1,2,4-triazolo[4,3-*a*]quinoxalin-1-one derivatives as A_1 and A_3 adenosine receptor antagonists. *Arch. Pharm. (Weinheim, Ger.)* **2004**, *337*, 35–41.
(19) Colotta, V.; Catarzi, D.; Varano, F.; Calabri, F. R.; Lenzi, O.; Filacchioni, G.; Trincavelli, L.; Martini, C.; Deflorian, F.; Moro, S. 1,2,4-Triazolo[4,3-*a*]quinoxalin-1-one moiety as an attractive scaffold to develop new potent and selective human A_3 adenosine receptor antagonists: synthesis, pharmacological and ligand-receptor modeling studies. *J. Med. Chem.* **2004**, *47*, 3580–3590.
(20) Catarzi, D.; Colotta, V.; Varano, F.; Calabri, F. R.; Lenzi, O.; Filacchioni, G.; Trincavelli, L.; Martini, C.; Tralli, A.; Montopoli, C.; Moro, S. 2-Aryl-8-chloro-1,2,4-triazolo[1,5-*a*]quinoxalin-4-amines as highly potent A_1 and A_3 adenosine receptor antagonists. *Bioorg. Med. Chem.* **2005**, *13*, 705–715.
(21) Catarzi, D.; Colotta, V.; Varano, F.; Lenzi, O.; Filacchioni, G.; Trincavelli, L.; Martini, C.; Montopoli, C.; Moro, S. 1,2,4-Triazolo[1,5-*a*]quinoxaline as a versatile tool for the design of selective human A_3 adenosine receptor antagonists: synthesis, biological evaluation and molecular modeling studies of 2-(hetero)aryl- and 2-carboxy-substituted derivatives. *J. Med. Chem.* **2005**, *48*, 7932–7945.
(22) Lenzi, O.; Colotta, V.; Catarzi, D.; Varano, F.; Filacchioni, G.; Martini, C.; Trincavelli, L.; Ciampi, O.; Varani, K.; Marighetti, F.; Morizzo, E.; Moro, S. 4-Amido-2-aryl-1,2,4-triazolo[4,3-*a*]quinoxalin-1-ones as new potent and selective human A_3 adenosine receptor antagonists. Synthesis, pharmacological evaluation and ligand−receptor modeling studies. *J. Med. Chem.* **2006**, *49*, 3916–3925.
(23) Morizzo, E.; Capelli, F.; Lenzi, O.; Catarzi, D.; Varano, F.; Filacchioni, G.; Vincenzi, F.; Varani, K.; Borea, P. A.; Colotta, V.; Moro, S. Scouting human A_3 adenosine receptor antagonist binding mode using a molecular simplification approach: from triazoloquinoxaline to a pyrimidine skeleton as a key study. *J. Med. Chem.* **2007**, *50*, 6596–6606.
(24) Colotta, V.; Catarzi, D.; Varano, F.; Lenzi, O.; Filacchioni, G.; Martini, C.; Trincavelli, L.; Ciampi, O.; Traini, C.; Pugliese, A. M.; Pedata, F.; Morizzo, E.; Moro, S. Synthesis, ligand−receptor modeling studies and pharmacological evaluation of novel 4-modified 1,2,4-triazolo[4,3-*a*]quinoxalin-1-one derivatives as potent and selective human A_3 adenosine receptor antagonists. *Bioorg. Med. Chem.* **2008**, *16*, 6086–6102.
(25) Shawali, A. S.; Albar, H. A. Kinetics and mechanism of dehydrochlorination of *N*-aryl-*C*-ethoxycarbonylformohydrazidoyl chlorides. *Can. J. Chem.* **1986**, *64*, 871–875.
(26) Lozinskii, M. O.; Kukota, S. N.; Pel'kis, P. S. Ethyl arylazochloroacetates and their reactions with morpholine and hydrazine hydrate. *Ukr. Khim. Zh.* **1967**, *33*, 1295–1296. [*Chem. Abstr.* **1968**, *69*, 51762].
(27) Cardia, M. C.; Corda, L.; Fadda, A. M.; Maccioni, A. M.; Maccioni, E.; Plumitallo, A. New cycloalkylpyrazoles as potential cyclooxygenase inhibitors. *Farmaco* **1998**, *53*, 698–708.
(28) Moro, S.; Deflorian, F.; Spalluto, G.; Pastorin, G.; Cacciari, B.; Kim, S.-K.; Jacobson, K. A. Demystifying the three dimensional structure of G protein-coupled receptors (GPCRs) with the aid of molecular modeling. *Chem. Commun. (Cambridge, U.K.)* **2003**, *24*, 2949–2956.
(29) Moro, S.; Spalluto, G.; Jacobson, K. A. Techniques: recent developments in computer-aided engineering of GPCR ligands using the human A_3 adenosine receptor as an example. *Trends Pharmacol. Sci.* **2005**, *26*, 44–51.
(30) Moro, S.; Deflorian, F.; Bacilieri, M.; Spalluto, G. Novel strategies for the design of new potent and selective human A_3 receptor antagonists: an update. *Curr. Med. Chem.* **2006**, *13*, 639–645.
(31) Moro, S.; Bacilieri, M.; Deflorian, F.; Spalluto, G. G protein-coupled receptors as challenging druggable targets: insights from in silico studies. *New J. Chem.* **2006**, *30*, 301–308.
(32) Cherezov, V.; Rosenbaum, D.; Hanson, M.; Rasmussen, S.; Thian, F.; Kobilka, T.; Choi, H.; Kuhn, P.; Weis, W.; Kobilka, B.; Stevens, R. High-resolution crystal structure of an engineered human beta2-adrenergic G protein-coupled receptor. *Science* **2007**, *318*, 1258–1265.
(33) Warne, T.; Serrano-Vega, M. J.; Baker, J. G.; Moukhametzianov, R.; Edwards, P. C.; Henderson, R.; Leslie, A. G.; Tate, C. G.; Schertler, G. F. Structure of a beta1-adrenergic G-protein-coupled receptor. *Nature* **2008**, *454*, 486–491.
(34) Jaakola, V.; Griffith, M.; Hanson, M.; Cherezov, V.; Chien, E.; Lane, J.; IJzerman, A.; Stevens, R. The 2.6 angstrom crystal structure of a human A_{2A} adenosine receptor bound to an antagonist. *Science* **2008**, *322*, 1211–1217.
(35) Moro, S.; Deflorian, F.; Bacilieri, M.; Spalluto, G. Ligand-based homology modeling as attractive tool to inspect GPCR structural plasticity. *Curr. Pharm. Des.* **2006**, *12*, 2175–2185.
(36) Ballesteros, J. A.; Weinstein, H. Integrated methods for modeling G-protein coupled receptors. *Methods Neurosci.* **1995**, *25*, 366–428.
(37) Somjen, G. G. Mechanisms of spreading depression and hypoxic spreading depression-like depolarization. *Physiol. Rev.* **2001**, *81*, 1065–1096.
(38) Latini, S.; Bordoni, F.; Pedata, F.; Corradetti, R. Extracellular adenosine concentrations during in vivo ischemia in rat hippocampal slices. *Br. J. Pharmacol.* **1999**, *127*, 729–739.
(39) Pearson, T.; Damian, K.; Lynas, R. E.; Frenguelli, B. G. Sustained elevation of extracellular adenosine and activation of A_1 receptors underlie the post-ischaemic inhibition of neuronal function in rat hippocampus in vitro. *J. Neurochem.* **2006**, *97*, 1357–1368.
(40) *MOE (The Molecular Operating Environment)*, version 2006.08, software available from Chemical Computing Group Inc., 1010 Sherbrooke Street West, Suite 910, Montreal, Canada H3A 2R7. http://www.chemcomp.com.
(41) Stewart, J. J. P. *MOPAC*, version 7; Fujitsu Limited: Tokyo, Japan, 1993.
(42) Palczewski, K.; Kumasaka, T.; Hori, T.; Behnke, C. A.; Motoshima, H.; et al. Crystal structure of rhodopsin: A G protein-coupled receptor. *Science* **2000**, *289*, 739–745.
(43) Cornell, W. D.; Cieplak, P.; Bayly, C. I.; Gould, I. R.; Merz, K. M.; Ferguson, D. M.; Spellmeyer, D. C.; Fox, T.; Caldwell, J. W.; Kollman, P. A. A second generation force field for the simulation of proteins, nucleic acids and organic molecules. *J. Am. Chem. Soc.* **1995**, *117*, 5179–5196.
(44) Levitt, M. Accurate modeling of protein conformation by automatic segment matching. *J. Mol. Biol.* **1992**, *226*, 507–533.
(45) Baxter, C. A.; Murray, C. W.; Clark, D. E.; Westhead, D. R.; Eldridge, M. D. Flexible docking using Tabù search and an empirical estimate of binding affinity. *Proteins: Struct., Funct., Genet.* **1998**, *33*, 367–382.
(46) Halgren, T. Merck molecular force field. I. Basis, form, scope, parameterization, and performance of MMFF94. *J. Comput. Chem.* **1996**, *17*, 490–519.
(47) Manetti, F.; Schenone, S.; Bondavalli, F.; Brullo, C.; Bruno, O.; Ranise, A.; Mosti, L.; Menozzi, G.; Fossa, P.; Trincavelli, M. L.; Martini, C.;

Martinelli, A.; Tintori, C.; Botta, M. Synthesis and 3D QSAR of new pyrazolo[3,4-*b*]pyridines: potent and selective inhibitors of A_1 adenosine receptors. *J. Med. Chem.* **2005**, *48*, 7172–7185.

(48) Colotta, V.; Catarzi, D.; Varano, F.; Melani, F.; Filacchioni, G.; Cecchi, L.; Trincavelli, L.; Martini, C.; Lucacchini, A. Synthesis and A_1 and A_{2A} adenosine binding activity of some pyrano[2,3-*c*]pyrazol-4-ones. *Farmaco* **1998**, *53*, 189–196.

(49) Novellino, E.; Cosimelli, B.; Ehlardo, M.; Greco, G.; Iadanza, M.; Lavecchia, A.; Rimoli, M. G.; Sala, A.; Da Settimo, A.; Primofiore, G.; Da Settimo, F.; Taliani, S.; La Motta, C.; Klotz, K.-N.; Tuscano, D.; Trincavelli, M. L.; Martini, C. 2-(Benzimidazol-2-yl)quinoxalines: a novel class of selective antagonists at human A(1) and A(3) adenosine receptors designed by 3D database searching. *J. Med. Chem.* **2005**, *48*, 8253–8260.

(50) Klotz, K.-N.; Vogt, H.; Tawfik-Schlieper, H. Comparison of A_1 adenosine receptors in brain from different species by radioligand binding and photoaffinity labelling. *Naunyn Schmiedeberg's Arch. Pharmacol.* **1991**, *343*, 196–201.

(51) Nordstedt, C; Fredholm, B. A modification of a protein-binding method for rapid quantification of cAMP in cell-culture supernatants and body fluid. *Anal. Biochem.* **1990**, *189*, 231–234.

(52) Cheng, Y. C.; Prusoff, W. H. Relation between the inhibition constant K_i and the concentration of inhibitor which causes fifty percent inhibition (IC_{50}) of an enzyme reaction. *Biochem. Pharmacol.* **1973**, *22*, 3099–3108.

(53) Anderson, W. W.; Collingridge, G. L. The LTP program: a data acquisition program for on-line analysis of long-term potentiation and other synaptic events. *J. Neurosci. Methods* **2001**, *108*, 71–83.

(54) Farkas, E.; Pratt, R.; Sengpiel, F.; Obrenovitch, T. P. Direct, live imaging of cortical spreading depression and anoxic depolarisation using a fluorescent, voltage-sensitive dye. *J. Cereb. Blood Flow Metab.* **2008**, *28*, 251–262.

(55) Pedata, F.; Latini, S.; Pugliese, A. M.; Pepeu, G. Investigations into the adenosine outflow from hippocampal slices evoked by ischemia-like conditions. *J. Neurochem.* **1993**, *61*, 284–289.

(56) Pugliese, A. M.; Latini, S.; Corradetti, R.; Pedata, F. Brief, repeated, oxygen−glucose deprivation episodes protect neurotransmission from a longer ischemic episode in the in vitro hippocampus: role of adenosine receptors. *Br. J. Pharmacol.* **2003**, *140*, 305–314.

JM8014876